



October 14, 2014

Emily Lloyd
Commissioner

Paul V. Rush, P.E.
Deputy Commissioner
Bureau of Water Supply
prush@dep.nyc.gov

465 Columbus Avenue
Valhalla, NY 10595
T: (845) 340-7800
F: (845) 334-7175

Pamela Young, Ph.D.
New York State Department of Health
Bureau of Public Water Supply Protection
Empire State Plaza – Corning Tower 11th Floor
Albany, NY 12237

Phil Sweeney
United States Environmental Protection Agency - Region II
290 Broadway - 24th Floor
New York, NY 10007-1866

Dear Dr. Young and Mr. Sweeney:

Enclosed is the DEP Response to NYSDOH/USEPA Comments on FAD Deliverables submitted July 31, 2014, in accordance with the Revised 2007 Filtration Avoidance Determination (FAD).

As always, if you have any questions about these comments or other aspects of the City's watershed protection efforts, please do not hesitate to contact me.

Sincerely,

David S. Warne
Assistant Commissioner

**DEP Response to DOH/EPA Comments on the FAD Deliverable Reports
Submitted July 31, 2014**

Response Date October 14, 2014

4.2 Land Acquisition Program

The semi-annual report on the status and activities of the Land Acquisition Program was submitted as required by the 2007 Revised FAD. The report states that “the 2014 FAD imposes a minimum 250,000-acre solicitation goal that covers the five-year period inclusive of 2012-2016...” The 2007 Revised FAD actually states that NYCDEP must solicit at least 300,000 acres through 2017, with credit toward this goal given for acres solicited in 2012 and 2013.

DEP Response:

Comment noted.

NYSDOH/EPA acknowledges NYCDEP’s June 11, 2014 request to NYSDEC to modify NYC’s Water Supply Permit to allow implementation of a City-funded Flood Buy-Out Program. The submission satisfies the 2007 Revised FAD requirement to submit such request.

DEP Response:

Comment noted.

4.8 Wetlands Protection Program

A report on the status of analysis of reference wetlands data and development of reference standards was submitted as required by the 2007 Revised FAD. The report is a well-organized and concise summary of the extensive data collected at NYCDEP’s 19 reference wetlands in the WOH watershed. The report notes that a wider geographic distribution of reference wetlands “would enable a more thorough characterization of the Catskill and Delaware watersheds...” Does NYCDEP feel that adding reference wetlands would be a worthwhile enhancement to the program? While reporting on the use of the reference wetland data is not within the scope of the report, NYSDOH is interested in hearing (perhaps in the FAD annual report) about examples where NYCDEP has been able to apply data from the reference wetlands, e.g., to help inform a wetlands mitigation project.

DEP Response:

DEP’s reference wetlands program provides a richer source of data than is available for many other geographic regions and is a thorough characterization of forested wetlands of the Catskill and Delaware Watersheds. However, comparing the distribution of reference and National Wetland Inventory wetlands indicates that emergent reference sites are underrepresented in the Schoharie, Cannonsville, Pepacton, and Rondout basins. While addition of emergent reference wetlands would provide enhanced regional baseline and long-term data, it may not be required to achieve mitigation goals, as emergent wetlands have proven easier to create than their forested counterparts (National Research Council, 2001, Compensating for Wetland Losses under the Clean Water Act). In considering whether to add reference wetlands, DEP will balance its long term goals and needs for this study against existing program efforts.

DEP has applied data from its reference wetland program to several mitigation projects and will provide a summary of these efforts in the FAD annual report.

4.11 Catskill Turbidity Control Program

A summary report on Catskill Turbidity Control measures was submitted in accordance with the 2007 Revised FAD. As required by the FAD, the report provides a concise summary of the costs, feasibility, and potential effectiveness of turbidity control measures that were considered by the Phase II and III Catskill Turbidity Control Studies and the 2008 Value Engineering review. In addition, the report summarizes the turbidity control measures that will be assessed in the environmental review being conducted in relation to the proposed modification to NYCDEP's Catalum SPDES permit. NYSDOH notes that the report is well written, and serves as a useful reference for reviewing NYCDEP's efforts towards investigating turbidity control measures.

DEP Response:

Comment noted.

5.1 Watershed Monitoring Program

The 2013 Watershed Water Quality Annual Report (the Report) is a comprehensive summary of the monitoring, modeling, and research conducted by NYCDEP pursuant to its watershed protection program. NYSDOH notes in particular that the quality of the data presentation and format of the Report result in a concise delivery of information that is also "reader-friendly." The Report also describes the scientific studies being conducted in the watershed, both by NYCDEP staff and through other professional research collaborations. The list of peer-reviewed publications included in the Report attests to the quality of this research. NYSDOH has noted the Report's acknowledgment section and concurs that the pride mentioned is an important fundamental to the success of NYC's watershed protection programs; we commend NYCDEP for setting and maintaining high standards in its work.

DEP Response:

Comment noted.

NYSDOH/EPA have the following additional comments/questions on this report:

The Report would benefit from including a list of acronyms.

DEP Response:

DEP will include a "List of Acronyms" in future reports.

In Section 1.1.2, NYSDOH/EPA note the planned deployment of additional profiling buoys in the RoboMon program. We also note the expected deployment of under-ice buoys in the Ashokan Reservoir for the 2014-15 winter season. Successful operation at Ashokan may allow for expansion into the Kensico Reservoir in future years.

DEP Response:

Comment noted.

Section 3.1.1 discusses the seiche observed in the Schoharie Reservoir between July and September 2013. A report from the Upstate Freshwater Institute is referenced in this section. We would be interested in receiving a copy of this report. Does DEP plan to collaborate with UFI on additional modeling of turbidity and temperature oscillations in the Schoharie, to include data from the 2014 occurrence?

DEP Response:

It is anticipated that further work on the Schoharie seiche issue with UFI will be performed under an OST continuing support contract that is currently being developed by DEP. This work would use a resuspension algorithm in the CEQUAL-W2 model with some additional calibration to attempt to correct for the sub-daily oscillations in the withdrawal turbidity. The timing of temperature oscillations due to the seiche are generally already well simulated by the model.

A copy of Upstate Freshwater Institute report "Short-term Variations in Temperature and Turbidity at Shandaken Tunnel Intake: Internal Wave Activity in Schoharie Reservoir" is attached.

In Section 5, the discussion on pathogens should include information on the matrix spike recoveries, either in aggregate for the year, broken down into each reporting section or added to Tables 5.6, 5.7, and 5.8. This quality control information would help provide context for the reported pathogen detections and summary statistics.

DEP Response:

DEP will add matrix spike recovery data to the pathogen tables in future reports.

In Section 7.1.4, the text mentions the USGS turbidity monitoring study on the Esopus, and refers to a final report. We would be interested in receiving a copy of this report.

DEP Response:

At this time, the report is under internal review by USGS. DEP will forward a copy of this report to reviewers once the report is final.

The first part of the report deals with the general situation of the country and the position of the various groups. It is followed by a detailed account of the events of the past few days, and a summary of the results of the operations.

The operations of the past few days have been successful in many respects. The main objective of the operations was to secure the safety of the population and to restore order to the country. This has been achieved in a large measure, and the situation is now more stable than it has been for some time.

The operations have also resulted in the capture of a large number of weapons and ammunition. These have been destroyed, and the remaining stores have been placed in a secure location. This will help to prevent the weapons from falling into the hands of the enemy.

The operations have also resulted in the capture of a large number of prisoners. These have been treated humanely, and their names and addresses have been recorded. They will be released as soon as possible, and their families will be notified.

The operations have also resulted in the capture of a large number of documents. These have been examined, and the information they contain has been used to identify the enemy's plans and intentions. This will help to prevent the enemy from carrying out their plans.

Final Report

Short-term Variations in Temperature and Turbidity at Shandaken Tunnel Intake: Internal Wave Activity in Schoharie Reservoir

Prepared by:
Upstate Freshwater Institute
Syracuse, NY

Prepared for:
New York City Department of Environmental Protection
Kingston, NY

January 2014

Table of Contents

1. Background and Goals.....	3
2. Observations and Evidence for Internal Waves	4
2.1. Shandaken Tunnel Data – 2013 and 2007–2012	4
2.2. In-Reservoir Data – 2013.....	9
2.3. Wind Data – 2007–2013	14
3. Internal Waves.....	17
3.1. Parameterization and Wedderburn Number.....	18
3.2. Example Calculations for a Wind Event	20
3.3. Observed Wave Period(s)	21
4. Modeling Analysis.....	23
4.1. Selected Inputs.....	23
4.2. Model Results	27
4.3. Analysis of Predicted Isotherms.....	28
4.4. Withdrawal Turbidity.....	35
5. Summary and Conclusions	38
6. References	39

1. Background and Goals

Schoharie Reservoir is located (latitude 42° 23.5' N; longitude 74° 27' W) in southern New York, approximately 190 km from New York City (NYC), and is operated by New York City Department of Environmental Protection (NYCDEP). This impoundment, initially filled in 1927, is part of a network of 19 reservoirs that supplies drinking water to 9 million people in the NYC area, contributing 16% of the total delivered. The reservoir is 8 km long, oriented along north-south axis, and lacks dendritic complexities (Figure 1). When full, the reservoir has a surface area of 4.0 km², a volume of 79 x 10⁶ m³, and a maximum depth of 40 m (Figure 1). The reservoir has a dimictic stratification regime. Its morphometric features often vary seasonally associated with the drawdown of the reservoir's surface (water surface elevation, WSE), in response to withdrawals for the water supply. Water withdrawn from it travels through a 29-km tunnel (Shandaken Tunnel), and then 20 km through a connecting Esopus Creek, before reaching the west basin of Ashokan Reservoir. Esopus Creek is a shallow stream that is influenced by Shandaken Tunnel discharge for both the flow and water quality, including temperature, during low flow periods.

The withdrawal is located at a depth of ~ 17 m, when full, in the upstream portion of the reservoir (Figure 1), and usually below the water layers that experience variations in temperature due to diurnal heating-cooling cycle. Examination of the temperature and turbidity data collected at the points of intake (SRR1) and the discharge (SRR2) in Shandaken Tunnel, from August 2013 reveals diurnal oscillations that suggest the presence of wind-induced internal waves (i.e., seiche). An analysis of the observations and modeling is conducted to further investigate the cause of the diurnal oscillations in withdrawal water temperature and turbidity.

Specific goals of this work were:

1. Document the oscillations observed in withdrawal temperature and turbidity during August 2013 at SRR1 and SRR2. Examine historical observations during periods of thermal stratification (typically, July–August) in the reservoir for recurrence of oscillations.
2. Analyze the wind data to determine the prominent wind directions during the July–August interval of 2007–2013.
3. Present a conceptual understanding of internal waves, describe a simple two-layer model of internal waves, and parameterize the model for a wind event at Schoharie Reservoir.
4. Compute periods of the internal waves from timeseries of temperature observations at SRR1.
5. Setup a previously validated 2-D model for Schoharie Reservoir for 2013, compare model predictions with the observations of in-reservoir and withdrawal T, and analyze selected isotherms for the presence of internal waves.

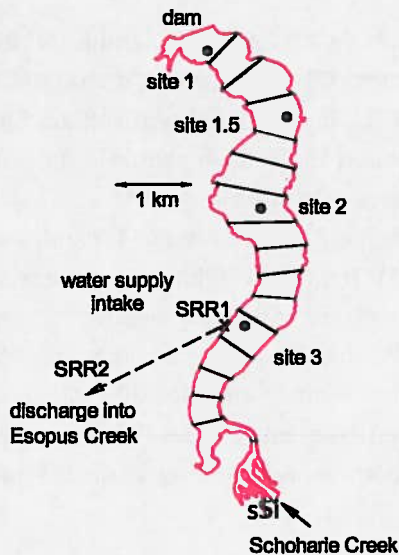


Figure 1. Schoharie Reservoir with withdrawal monitoring locations (SRR1 and SRR2), primary in-reservoir monitoring sites, and monitoring location on the primary tributary (Schoharie Creek; s5i). Longitudinal model segments are also indicated.

2. Observations and Evidence for Internal Waves

2.1. Shandaken Tunnel Data – 2013 and 2007–2012

NYCDEP monitors the withdrawal water quality at SRR1 and SRR2 routinely. In addition, USGS monitors the Shandaken Tunnel discharge rates and temperature at SRR2. Hourly observations of withdrawal temperature and turbidity made at SRR1 during August 2013 are shown in Figure 2. Diurnal oscillations of amplitude in excess of 5 °C and 75 NTU were observed in early-August, which gradually decreased later in the month. Similar patterns were also observed at SRR2 (Figure 3), indicating that the travel through the Tunnel has limited dampening effect on the amplitude of oscillations. While surface layers of the reservoir experience diurnal heating and cooling causing similar intra-day fluctuations in temperatures, no such systematic short-term variations are likely to occur in turbidity near the surface.

Historical temperature and turbidity at SRR1 were examined to find out if the diurnal oscillations are a recurring phenomenon in Schoharie Reservoir withdrawal. Timeseries of withdrawal temperature and turbidity, at SRR1 for August for 2007–2012, are presented in Figure 4 and Figure 5, respectively. Clearly, all of the years exhibited systematic diurnal oscillations in temperature and turbidity, although the magnitude of the diurnal swings varied from year to year. The factors that may influence the magnitude

of these oscillations are reservoir operation (i.e., drawdown and withdrawal rates), inflow regime of Schoharie Creek (i.e., underflow, interflow, or overflow), and wind speed and direction (amplitude of internal waves).

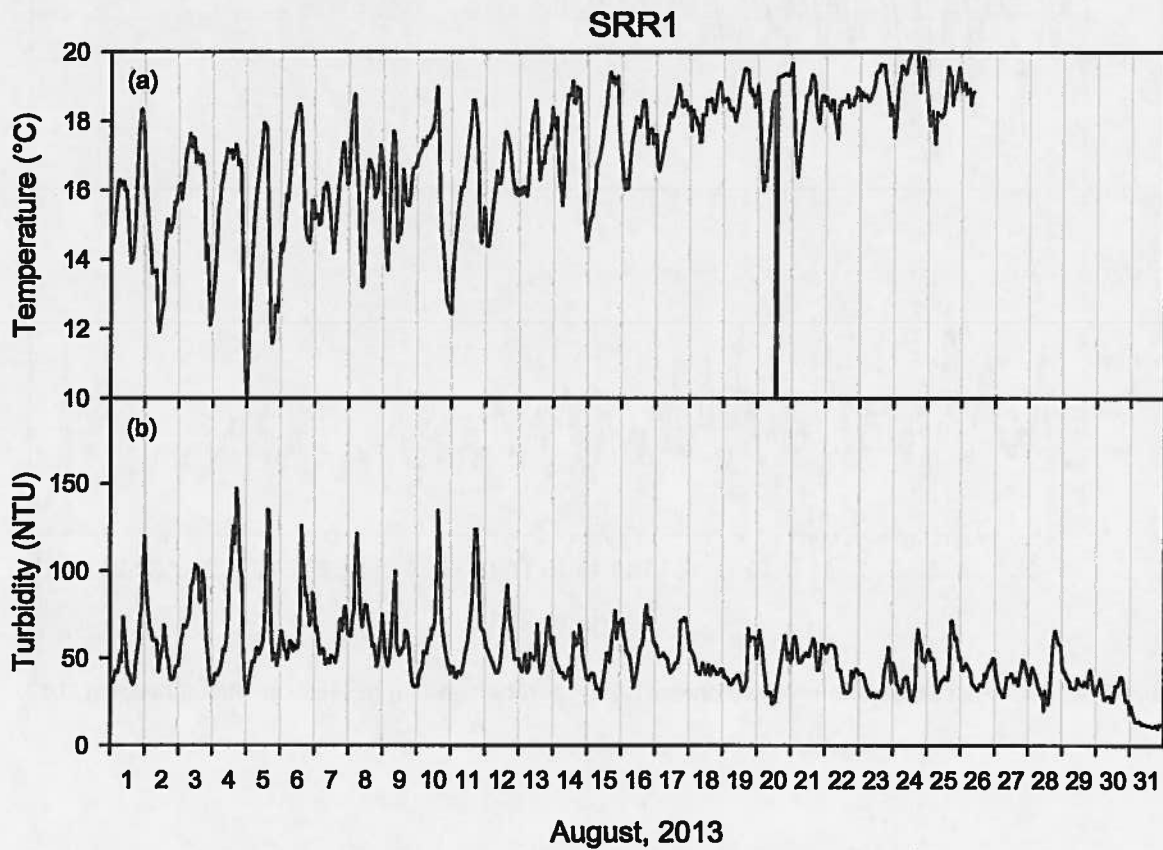


Figure 2. Timeseries of observations of withdrawal (a) temperature and (b) turbidity at SRR1 for August 2013.

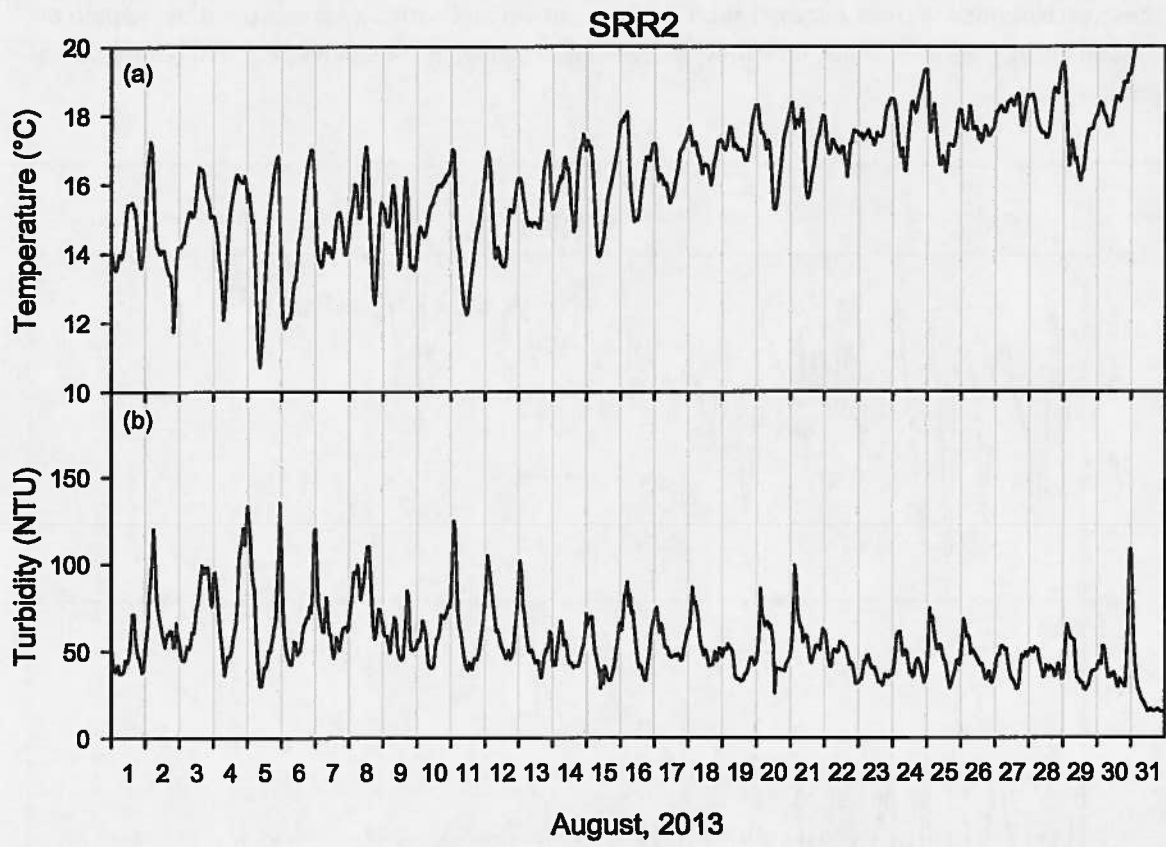


Figure 3. Timeseries of observations of withdrawal (a) temperature and (b) turbidity at SRR2 for August 2013.

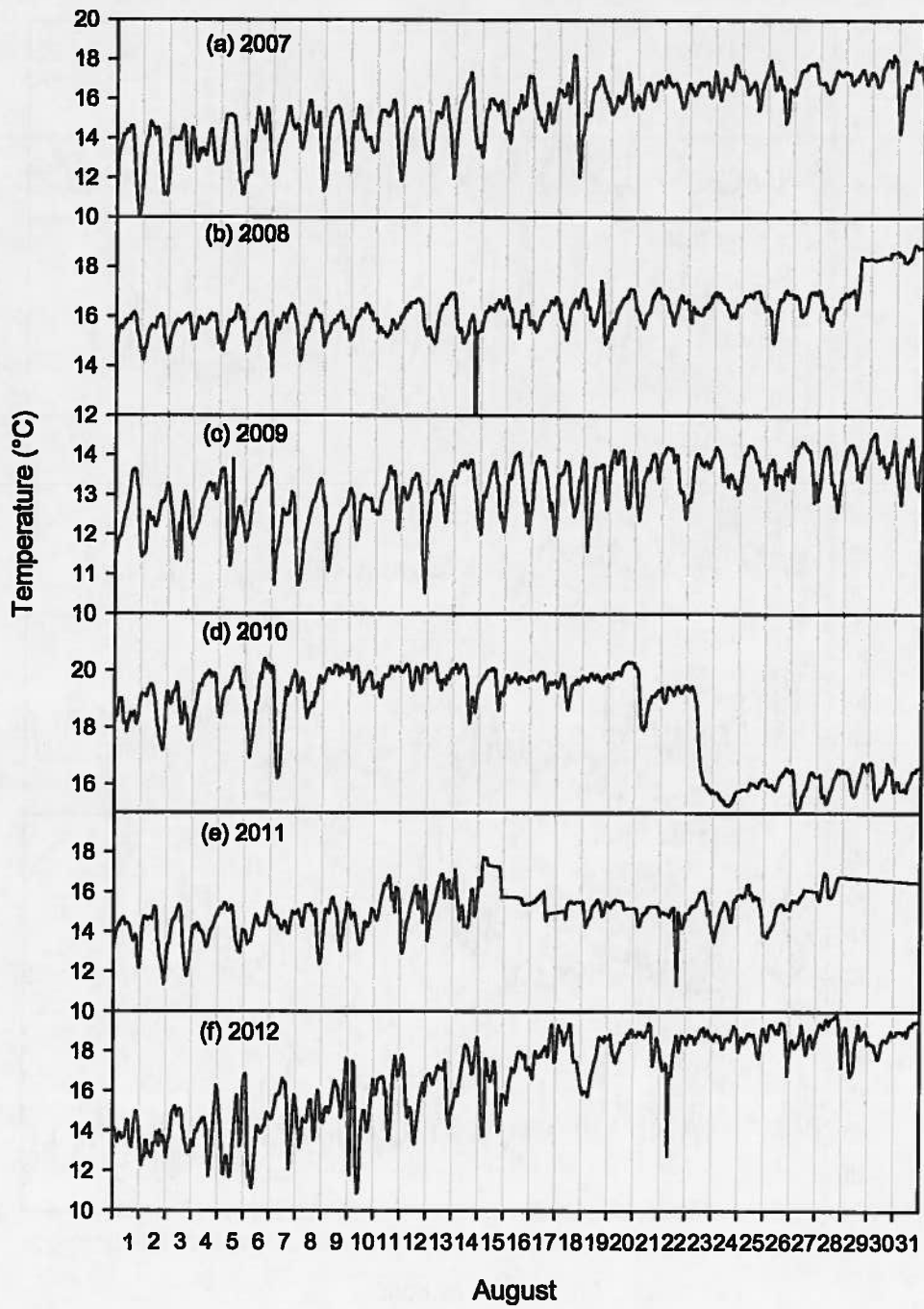


Figure 4. Timeseries of observations of withdrawal temperature at SRR1 for August, 2007–2013.

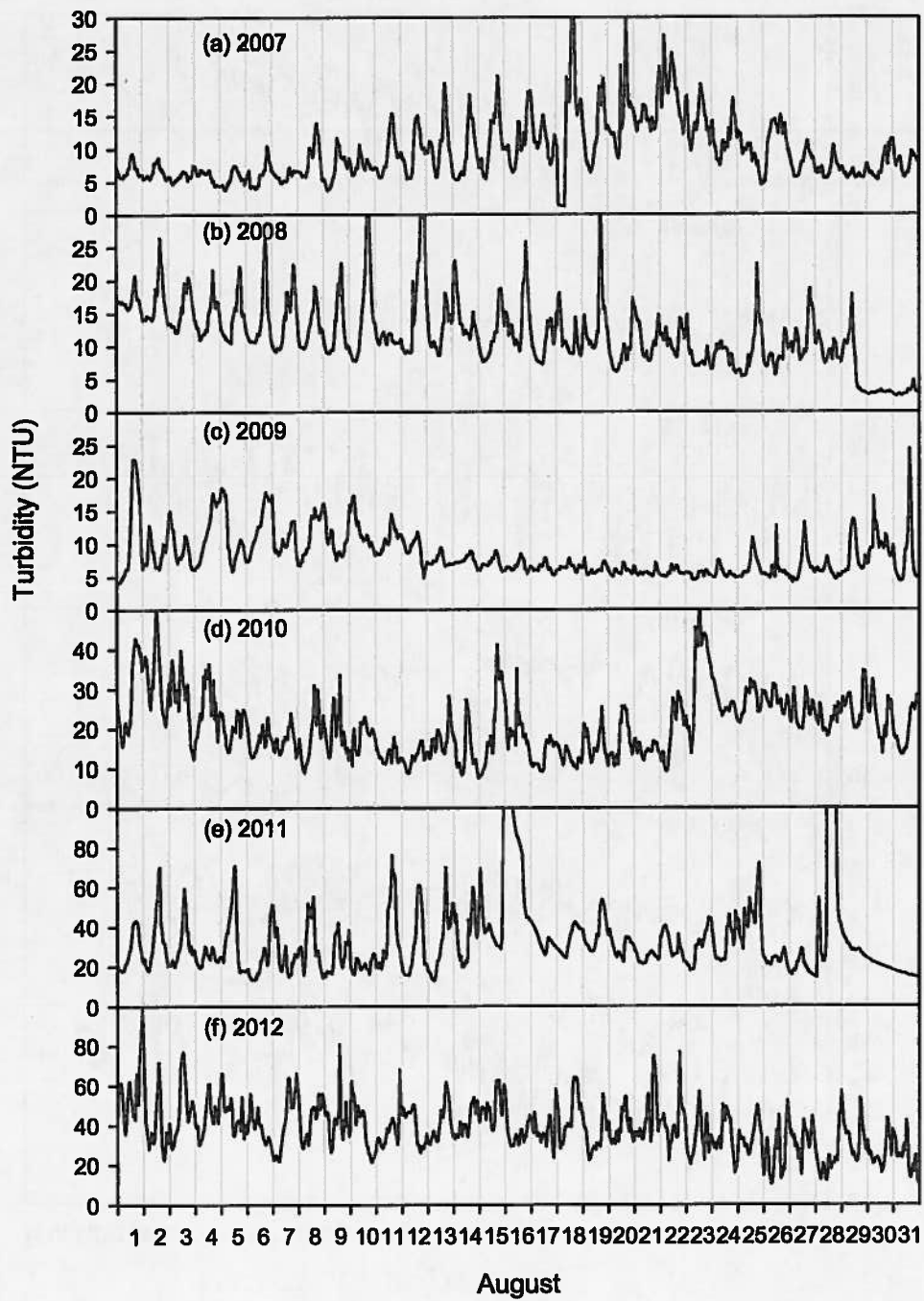


Figure 5. Timeseries of observations of withdrawal turbidity at SRR1 for August, 2007–2013.

2.2. In-Reservoir Data – 2013

Special monitoring surveys were conducted during August–September 2013, including deployment of thermistor chains at site 3 (Figure 1) by NYCDEP, to further explore the likely mechanisms of oscillatory patterns in withdrawal temperature and turbidity. Sampling locations for a special survey conducted on August 8, 2013 are shown in Figure 6. The survey included collection of depth-profiles of temperature (Figure 7) and turbidity (Figure 8) four times during the day at multiple locations, both longitudinally and laterally. Additional temperature profiles at every 3 hours at site 3 were also collected during September 4–September 7, 2013 (Figure 9).

Four temperature profiles at site 3 from August 22, 2013, indicate thermal stratification at that location, with the depth of the thermocline at ~ 13 m and the depth of the intake at 14.8 m (Figure 7a). Diurnal variations in temperature near the surface (0–3 m) due to solar heating and radiative cooling are observed (Figure 7a). Turbidity profiles also indicate stratification, with low values in the homogenous upper mixed layer (Figure 8a-c) and high values in the lower stratified layers. The stratification in turbidity may have developed from an underflow of a prior runoff event, resuspension driven by internal wave action, and settling of particles from upper waters.

Significant diurnal variations in both temperature (Figure 7a) and turbidity (Figure 8a) are also observed in water layers just below the thermocline (i.e., in the metalimnion) indicating the presence of internal wave. Inflow from Schoharie Creek could not have caused these variations as it was a low flow period (see Figure 18a) with likely low turbidity inputs (data not available). Lateral sites 3.02 and 3.03 are shallower than site 3 (Figure 6) and indicate similar surface layer diurnal temperature variations but no deep-water variations (Figure 7b, c). Stratification weakened further in September; however the deep-water diurnal oscillations in temperature persisted suggesting the continued operation of internal wave (Figure 9). Oscillations in temperature observations, as recorded by thermistor chains at sites 2 and 3, further provide the evidence for an internal wave in the reservoir (Figure 10).

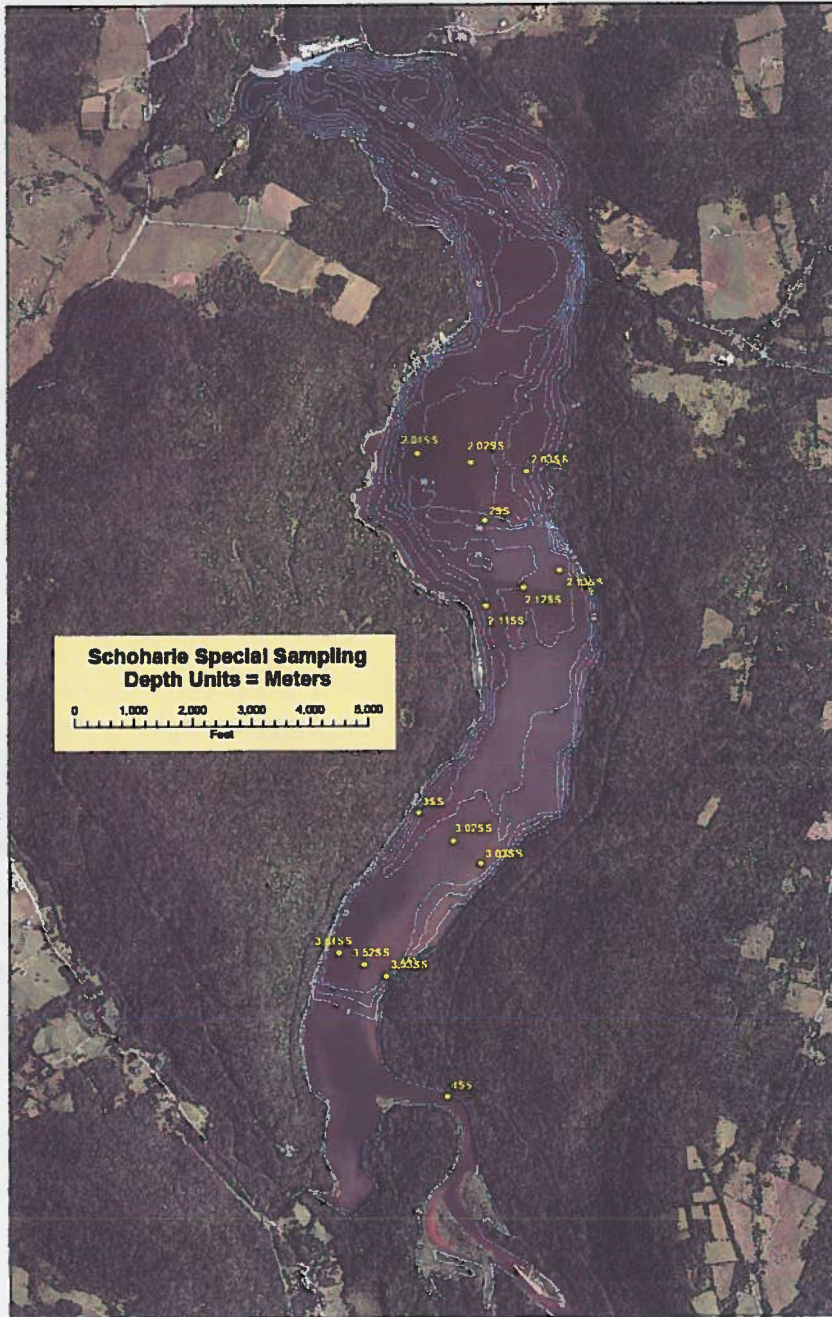


Figure 6. Locations of a special monitoring survey conducted on August 22, 2013, for Schoharie Reservoir.

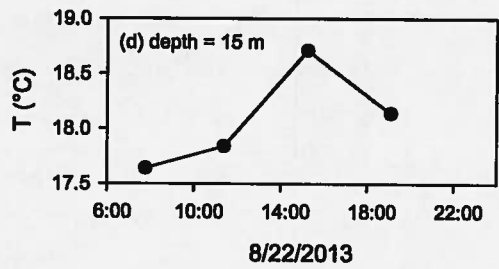
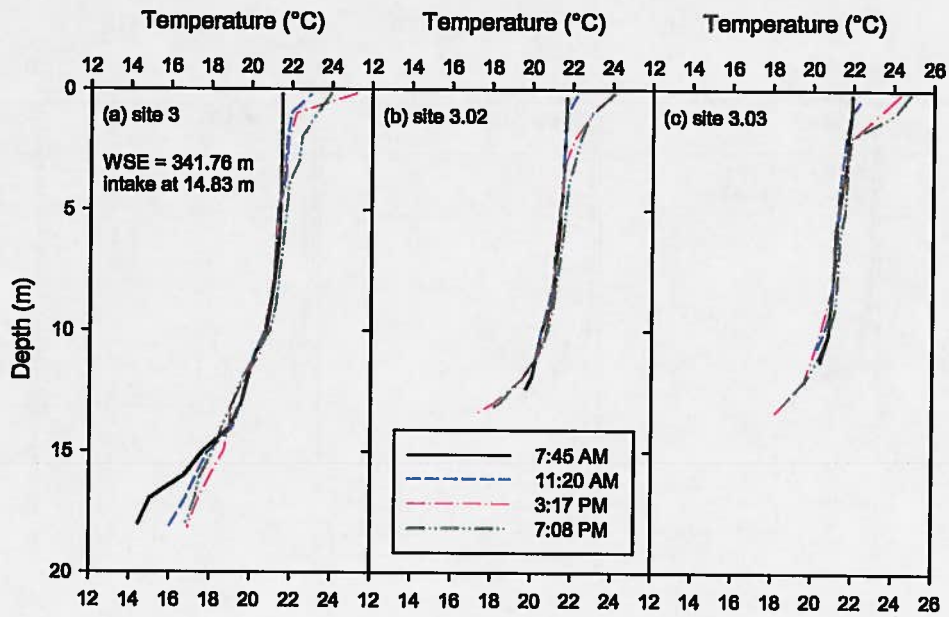


Figure 7. Observed temperature profiles for August 22, 2013 (n = 4), at (a) site 3, (b) site 3.02, and (c) site 3.03. Diurnal timeseries of temperature at a depth of 15 m, corresponding to the location of intake, is shown in (d).

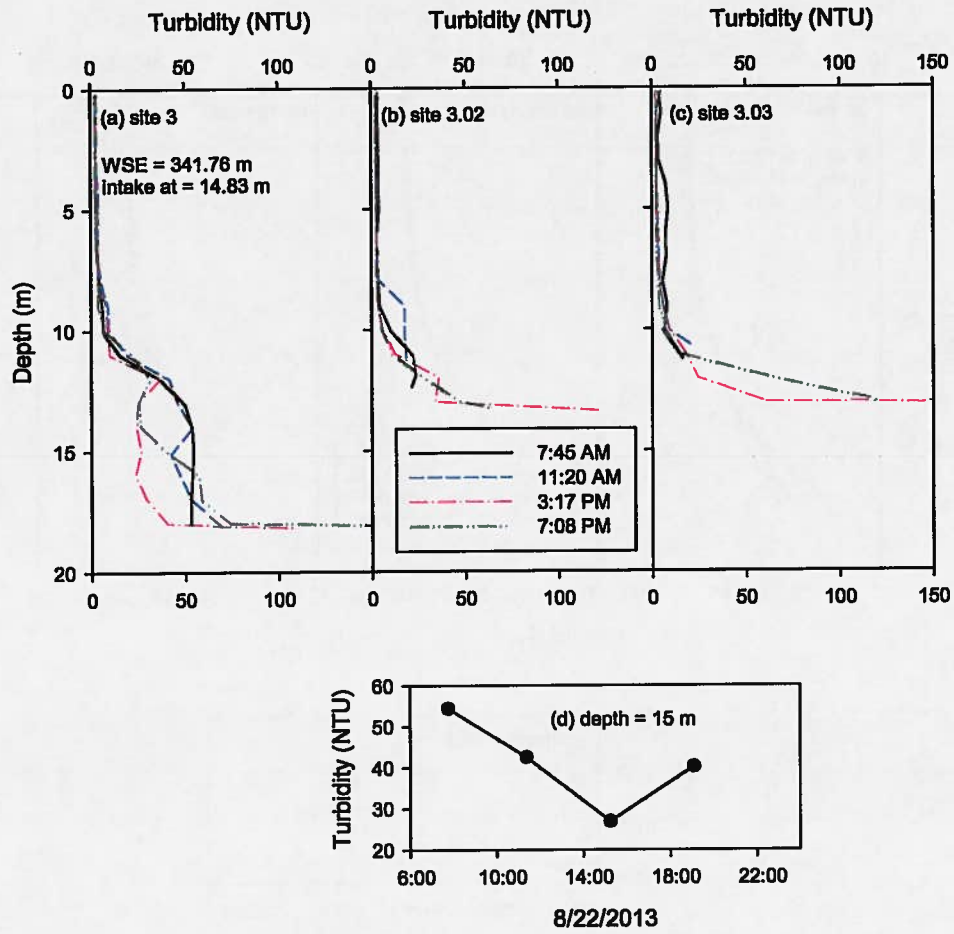


Figure 8. Observed turbidity profiles for August 22, 2013 ($n = 4$), at (a) site 3, (b) site 3.02, and (c) site 3.03. Diurnal timeseries of turbidity at a depth of 15 m, corresponding to the location of intake, is shown in (d).

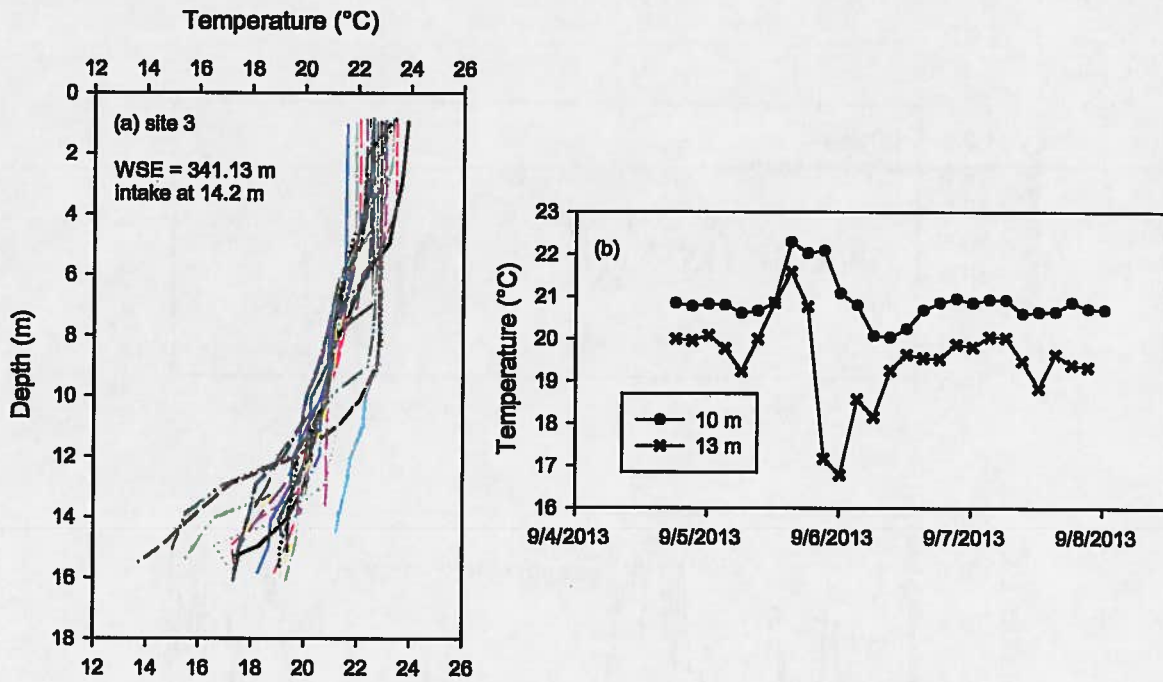


Figure 9. (a) Observed temperature profiles for September 4–September 7, 2013 (n = 27) at site 3, and (b) Diurnal timeseries of temperature at a depths of 10 m and 13 m.

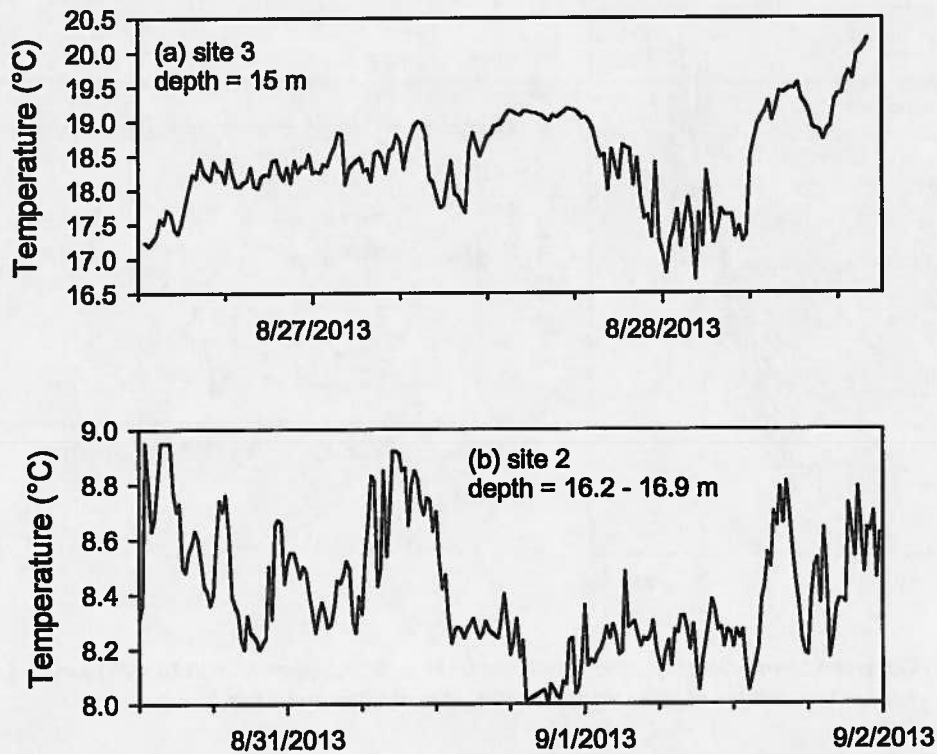


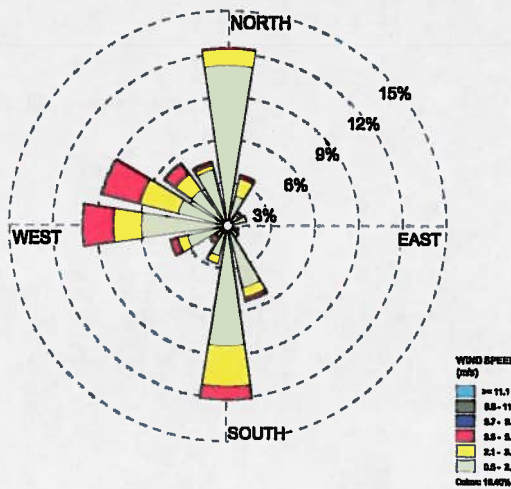
Figure 10. Observations of temperatures as measured by thermistor chains at (a) site 3 and (b) site 2, during August 26–September 2, 2013.

2.3. Wind Data - 2007–2013

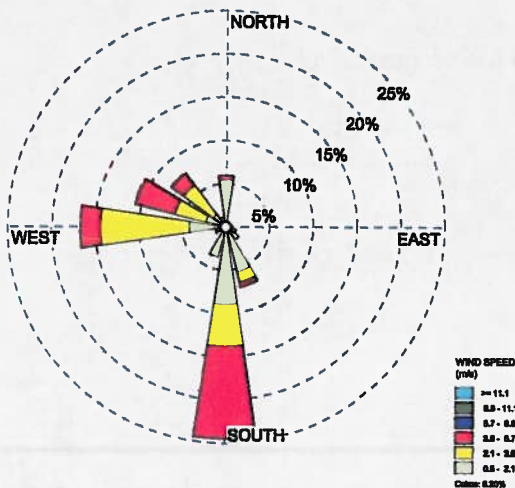
Wind is the fundamental driver for generating internal waves. Wind blowing along the main axis of a waterbody is more effective in transporting water at one end and disrupting the hydrostatic equilibrium (Wetzel 2001). Schoharie Reservoir is oriented along north-south direction in line with the prevailing winds blowing from either north or south directions. Wind data collected at a National Weather Service station located ~ 60 km away (northeast of the reservoir) at Albany, NY, were obtained and adjusted for the speed for onsite conditions (Upstate Freshwater Institute 2013). A frequency distribution analysis of the wind speed and direction data can be presented in the form of windrose plots. The windrose plots from 2007–2013 for July–August interval, as shown in Figure 11 and Figure 12, reveal that the predominant direction of the wind at Schoharie Reservoir is indeed along the primary axis of the reservoir.

Hourly wind speed from August 2013 was further examined for intensity, duration, and periodicity (Figure 13). The north-south component of wind speed obtained by multiplying the raw wind with the cosine of the observed direction is presented in Figure 13a, in which, positive values indicate wind blowing from north and negative values indicate wind blowing from south. Discernible features of this timeseries are (i) wind events of August 1 and August 7 with speeds of $\sim 4 \text{ m s}^{-1}$ from south that lasted for several hours, (ii) constantly shifting winds between north and south directions (Figure 13a). A spectral density analysis of these data identifies the underlying dominant periodicities as 6 d, 3.5 d, 2 d, and 1 d (Figure 13b). This repeated periodic north-south wind forcing provides the stress necessary for sustained internal waves in the reservoir.

(a) July, 2013



(b) August 1-7, 2013



(c) August 8-14, 2013

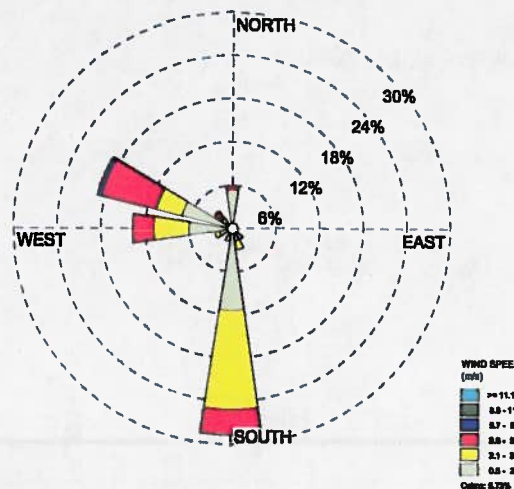
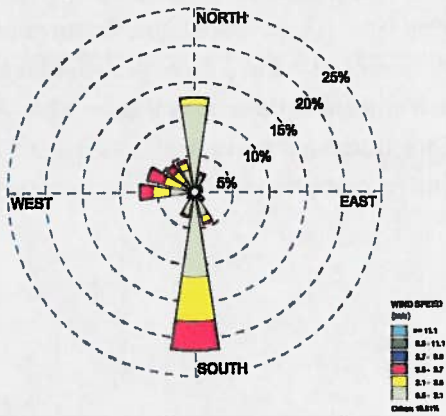
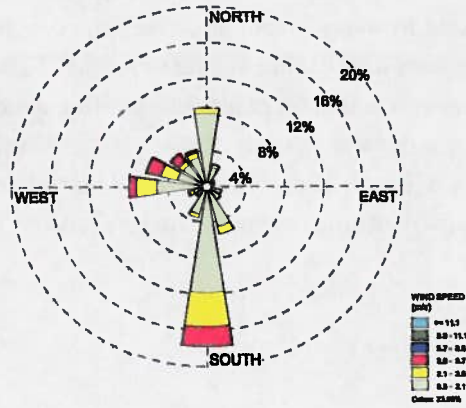


Figure 11. Windrose plots showing frequency distribution of wind speed and predominant wind directions for: (a) July, 2013, (b) first week of August, 2013, and (c) second week of August, 2013.

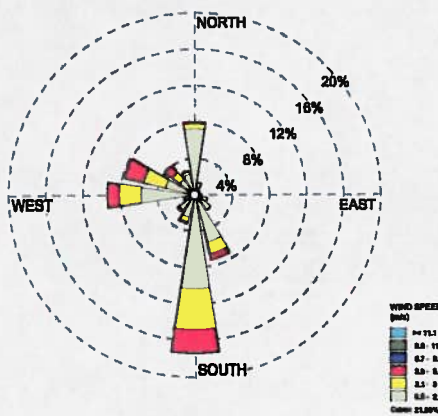
(a) July–August, 2007



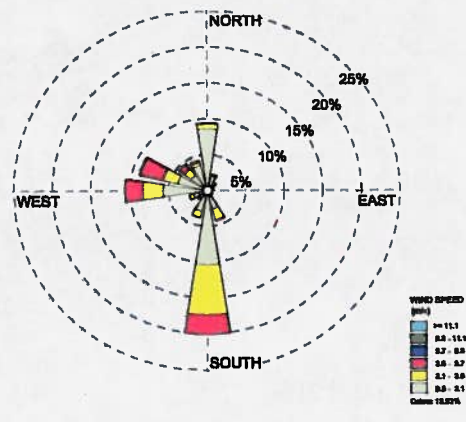
(b) July–August, 2008



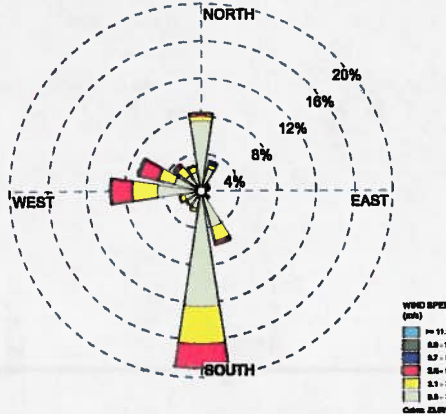
(c) July–August, 2009



(d) July–August, 2010



(e) July–August, 2011



(f) July–August, 2012

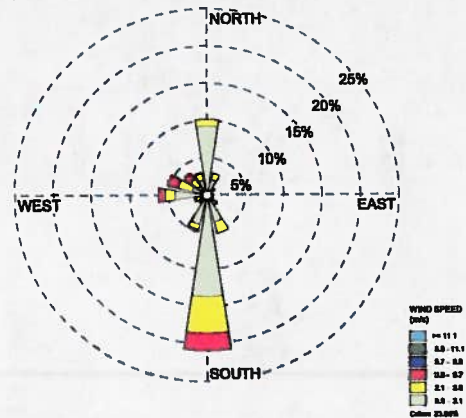


Figure 12. Windrose plots showing frequency distribution of wind speed and predominant wind directions for 2007–2012, for July–August intervals.

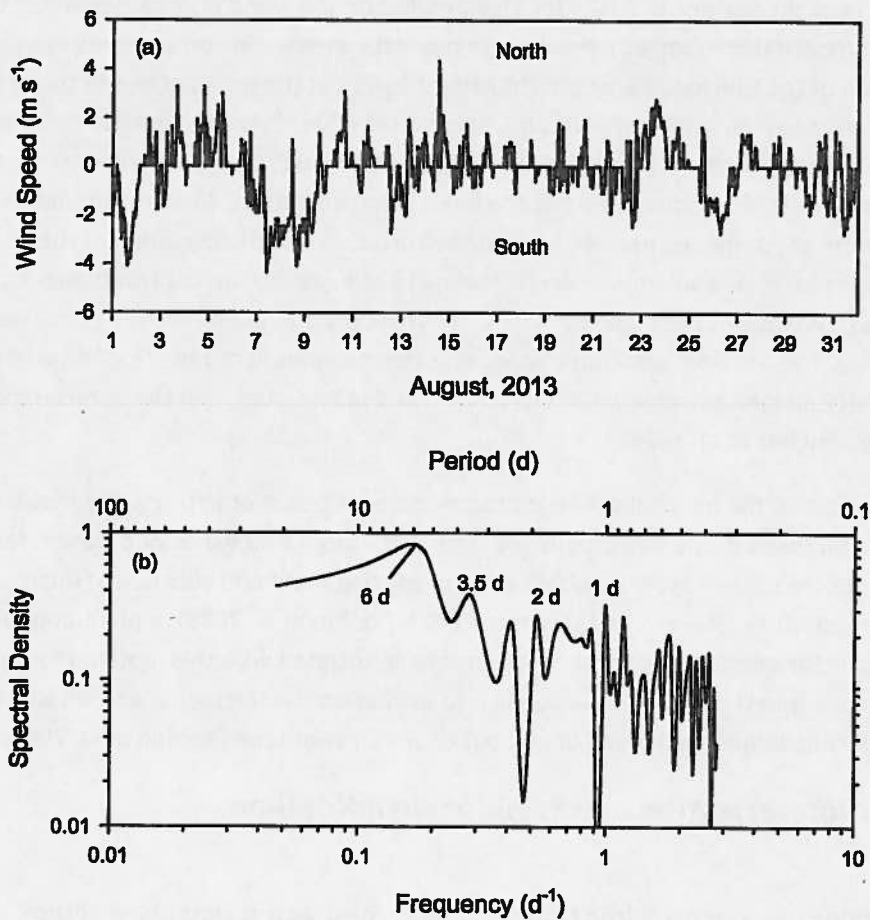


Figure 13. (a) Timeseries of wind speed along the main axis (north-south) of Schoharie Reservoir for August 2013, with a positive wind being from north, and (b) spectral density for wind speed in (a).

A conceptual discussion on what causes the internal waves is presented next. A simplified two-layer model is presented to parameterize the amplitude of these waves. Spectral analysis is used to quantify the frequency and period of these waves.

3. Internal Waves

Temperature fluctuations at the level of metalimnia have been observed widely (Wetzel 2001). Likewise, such fluctuations have also been observed in reservoir withdrawals (Carmack et al. 1986, Stevens and

Lawrence 1997, Anohin et al. 2006). These fluctuations have been directly linked to the wind stress at the surface of these lentic systems (Mortimer 1952, 1961).

As wind blows over the surface of a lake for an extended period, wind drift causes water to accumulate (Wetzel 2001, stress-induced set-up), resulting in modest increases in surface level, but potentially major expansion of the thermocline depth (Mortimer 1961), at the leeward end of the of the basin. This transport disrupts the hydrostatic equilibrium, and causes a 'tilt' in the pycnocline (layer of maximum density gradient) in a direction opposite to the surface slope, such that the minimum depth of the thermocline occurs at the windward end of the basin (Mortimer 1961, Martin and McCutcheon 1999), and the isotherms are deflected upward toward the surface. With the cessation of the wind the pycnocline begins to 'rock' and an internal (baroclinic) wave (seiche) across this boundary is introduced (Mortimer 1961). A wave of the uninodal type is the most predominant response of a lake to wind (Mortimer 1961). The 'rocking' can continue for an extended period of time (e.g., days) depending upon the morphometry, magnitude of wind-induced shear stress imparted, and the antecedent stratification conditions (e.g., Fischer et al. 1979).

An additional effect of the internal seiche is observed downstream or in the withdrawals of reservoirs when wind-driven thermocline deflections are sufficiently large that water of different temperature is moved to the depths of the reservoir withdrawal, producing rapid and substantial fluctuations in the withdrawal temperature (Stevens and Lawrence 1997, Anohin et al. 2006), a phenomenon observed here in Schoharie Reservoir withdrawal. Furthermore, associated with this motion of internal wave, any water quality constituent that is stratified, will also exhibit similar fluctuations in withdrawals as layers of different concentrations are moved in and out of withdrawal zone (Anohin et al. 2006).

3.1. Parameterization and Wedderburn Number

Parameterization of an internal seiche consists of quantifying two values: (i) the vertical displacement of the thermocline at the ends of the lake, and (ii) the time-scale for this response to occur. A simplified, two-layer (epilimnion and hypolimnion) system separated by an interface (the thermocline; i.e., infinitely sharp metalimnion) is considered (Figure 14). The degree of tilt of the base of the surface layer (epilimnion) resulting from an applied wind stress may be quantified using the dimensionless Wedderburn number (W ; Fischer et al. 1979, Monismith 1986), which as the ratio of the wind disturbance force to the gravitational baroclinic restoring force is given by

$$W = \frac{g' h_1^2}{L u_*^2} \quad (1)$$

where g' is the reduced gravity [$=g(\rho_2 - \rho_1)/\rho_2$; g is the gravitational constant, and ρ_1 and ρ_2 are the densities of the epilimnion and hypolimnion, respectively], h_1 is the thickness of the epilimnion, u_* is the

water shear velocity induced by the wind, and L is the characteristic length scale of the basin. The shear velocity, u_* , is estimated from the commonly used relationship (Martin and McCutcheon 1999):

$$u_* = C_d \frac{\rho_{air}}{\rho_1} U_{10}^2 \quad (2)$$

where ρ_{air} is the density of air (1.2 kg m^{-3}), U_{10} is the wind speed at 10 m above the surface of the reservoir, and C_d is the drag coefficient [1.3×10^{-3} ; for a moderate size lake (Fischer et al. 1979)]. Under the assumption that u_* acts evenly over the water surface and manifests itself as an evenly distributed force in the surface layer, the constant slope of the thermocline is given by Ri^{-1} ($Ri = h_1 g' / u_*^2$; Imberger 1985), and is required to offset the pressure gradient that opposes the wind stress. For small amplitude seiches the deflection or the tilt, η , can be determined from Ri and the surface layer aspect ratio h_1/L , so that (Imberger 1985, Stevens and Lawrence 1997):

$$\eta = \frac{L}{2Ri} \quad (3)$$

Combining Eqs. (1) and (3) results in

$$\eta = \frac{0.5h_1}{W} \quad (4)$$

If the wind is strong enough, upwelling occurs whereby the thermocline region reaches the surface at the upwind end ($W \approx 1$; e.g., Effler et al. 2004). For the two layer system considered here, the fundamental internal wave period is given by (e.g., Spigel and Imberger 1980):

$$T_1 = \frac{2L}{\sqrt{g' h_1 h_2 / (h_1 + h_2)}} \quad (5)$$

where, h_2 is the thickness of the hypolimnion. The time necessary for a perturbation at the middle of the lake to propagate along the principal axis to either boundary, and hence for a complete tilting of the pycnocline to occur is equal to $T_1/4$ (Spigel and Imberger 1980).

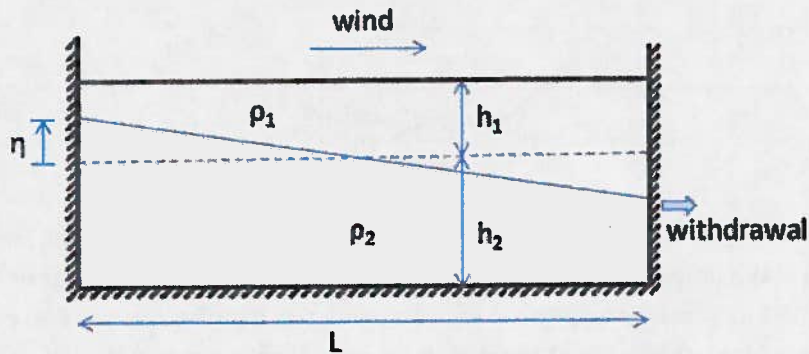


Figure 14. Illustration of an internal wave due to wind-setup in a two-layer model framework, including the withdrawal location (modified from Stevens and Lawrence 1997).

3.2. Example Calculations for a Wind Event

Calculations of the fundamental wave period T_1 , Wedderburn number W , and the maximum tilt of the pycnocline η , using the simple two-layer model [Eqs. (1)–(5)] are illustrated below for the wind event of August 7, 2013 (Figure 13). The average of the two temperature profiles from site 2, near the nodal point of the first mode internal wave, recorded on August 8, 2013 was used (Figure 15) to define the model parameters as follows:

h_1 = depth of pycnocline (maximum density gradient) = 11 m

h_2 = (mean depth of the region that is $> h_1$) – h_1 = 15.5 – 11 = 4.5 m

ρ_1 = density of the upper layer corresponding to h_1 , for average temperature of 21.65 °C = 997.852 kg m⁻³

ρ_2 = density of the lower layer corresponding to h_2 , for average temperature of 9.7 °C = 999.728 kg m⁻³

Additionally, the following values were adopted for other parameters:

L = characteristic length of the basin (at pycnocline) = 6400 m

U_{10} = wind speed at 10 m above the surface of the reservoir (= 1.26 U_2 ; White 1998) = 5 m s⁻¹

g = gravitational constant = 9.807 m s⁻²

ρ_{air} = density of air = 1.2 kg m⁻³

C_d = drag coefficient (Fischer et al. 1979) = 1.3×10^{-3}

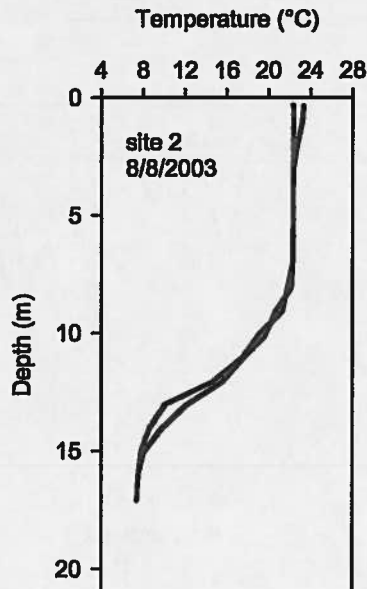


Figure 15. Depth-profiles of temperature observed on August 8, 2013 at site 2, following a wind event on August 7, 2013.

Substituting these values in Eqs. (1), (4) and (5) yields:

Wedderburn number, $W = 9$; tilt, $\eta = 63$ cm; and wave period, $T_1 = 14.7$ hr. $W \gg 1$ implies that the tilt of the pycnocline was not sufficient to reach the surface and cause upwelling in the reservoir for this wind event. The duration of wind necessary for the complete tilt of the pycnocline is $T_1/4 = 3.7$ hr.

3.3. Observed Wave Period(s)

A spectral analysis of the hourly timeseries of temperature observations at SRR1, for August 7-12, 2013 interval was conducted (Figure 16). The dominant periods of oscillations were found to be 22 hr and 14.5 hr (Figure 16). The two-layer model calculated period of 14.7 hr agreed well with one of the observed dominant periods. The other dominant period (22 hr) may indicate presence of other higher mode seiches in the reservoir. Spectral analysis of the hourly timeseries of temperature observations at SRR1 for another interval, August 1-6, 2013, revealed similar dominant periods of oscillations (22 hr and 15 hr; Figure 17).

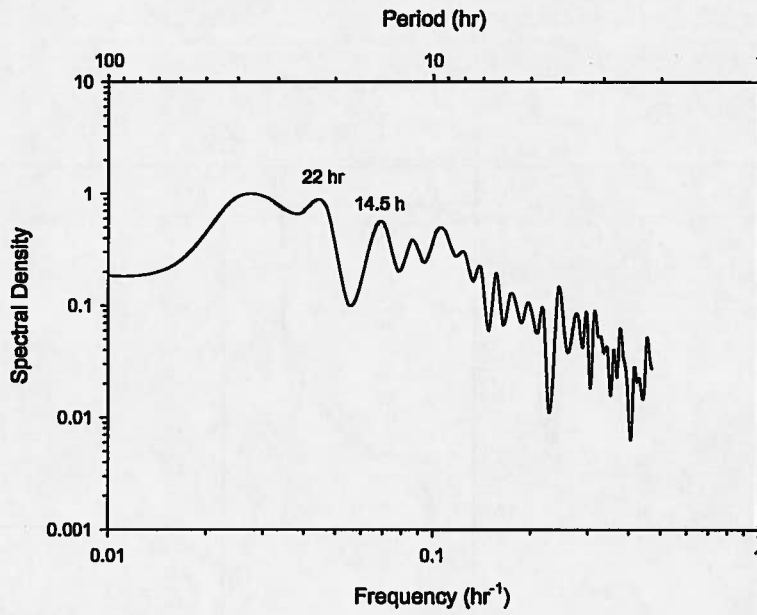


Figure 16. Spectra of timeseries of temperature observations in Shandaken Tunnel at SRR1 for the interval of August 7–August 12, 2013.

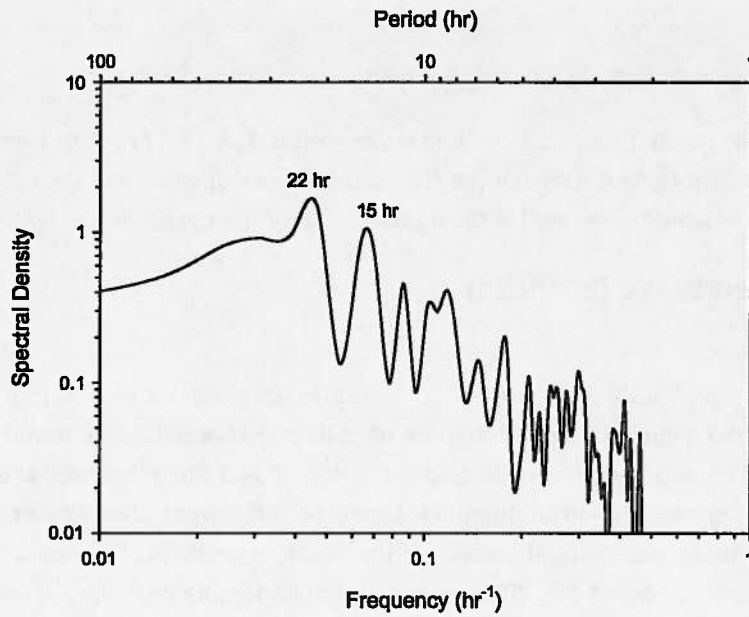


Figure 17. Spectra of timeseries of temperature observations in Shandaken Tunnel at SRR1 for the interval of August 1–August 6, 2013.

4. Modeling Analysis

A previously validated model (CE-QUAL-W2; subsequently identified as W2) for Schoharie Reservoir (Gelda and Effler 2007) was used to gain further insight into the formation of internal waves and their impact on withdrawal temperatures and turbidities. W2 is a dynamic, laterally averaged, two-dimensional (longitudinal-vertical) model (Cole and Wells 2011). The model represents the reservoir in the form of a grid of cells consisting of longitudinal segments and vertical layers. Modifications in this model setup from the earlier application were: (i) lower spillway elevation (1125 ft) as a result of the installation of a V-notch in Gilboa Dam, and (ii) siphoning of water from an elevation of 1104 ft from the model segment near the dam. It was assumed that the dredging done in the vicinity of the intake, after the previous modeling study was completed, did not alter the bathymetry significantly. Accordingly, no changes were made to the bathymetry file.

4.1. Selected Inputs

The model was setup for April–September 2013, with a focus on the July–August interval, a period of strong thermal stratification in the reservoir, and when substantial short-term (within a day) oscillations in the withdrawal temperature and turbidity were observed. Hydrological, and reservoir operations data, including Schoharie Creek inflow, Shandaken Tunnel withdrawal, Siphon outflow, spill, and water surface elevation for July–August, 2013 are presented in Figure 18.

Meteorological data were obtained from a National Weather Service station (located at Albany Airport, NY). These data were adjusted for the onsite conditions using regression relationships developed earlier with the onsite measurements (Upstate Freshwater Institute 2013), and specified as hourly inputs to the model (Figure 19). Detailed timeseries of meteorological inputs for August, 2013 are presented in Figure 20. Noteworthy features, as discussed earlier, are the periodic nature of wind speed primarily from the south direction and secondarily from the north direction, in alignment with the primary axis of the reservoir (Figure 20d-e).

Temperature of Schoharie Creek inflow was estimated at a frequency of once per hour from an empirical model based on stream flow and air temperature (Gelda and Effler 2008).

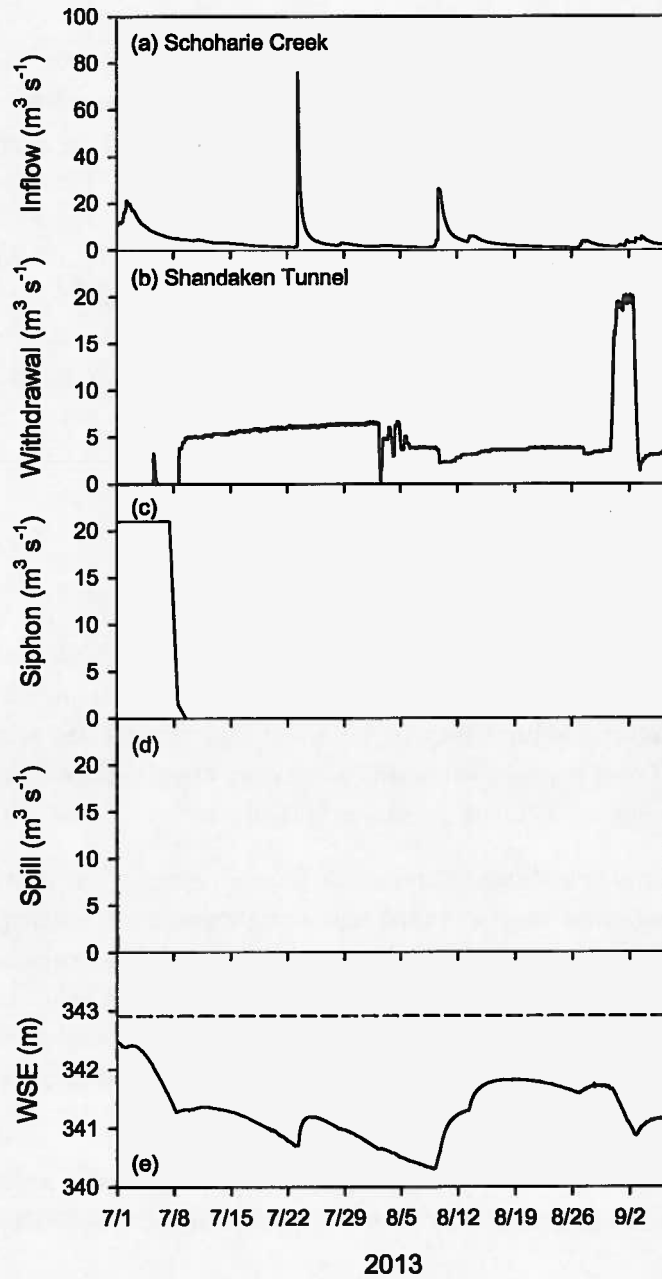


Figure 18. Hydrological and reservoir operations data for July–August, 2013: (a) inflow from Schoharie Creek, (b) withdrawal from the reservoir via Shandaken Tunnel, (c) outflow from the reservoir through siphons, (d) spill, and (e) water surface elevation.

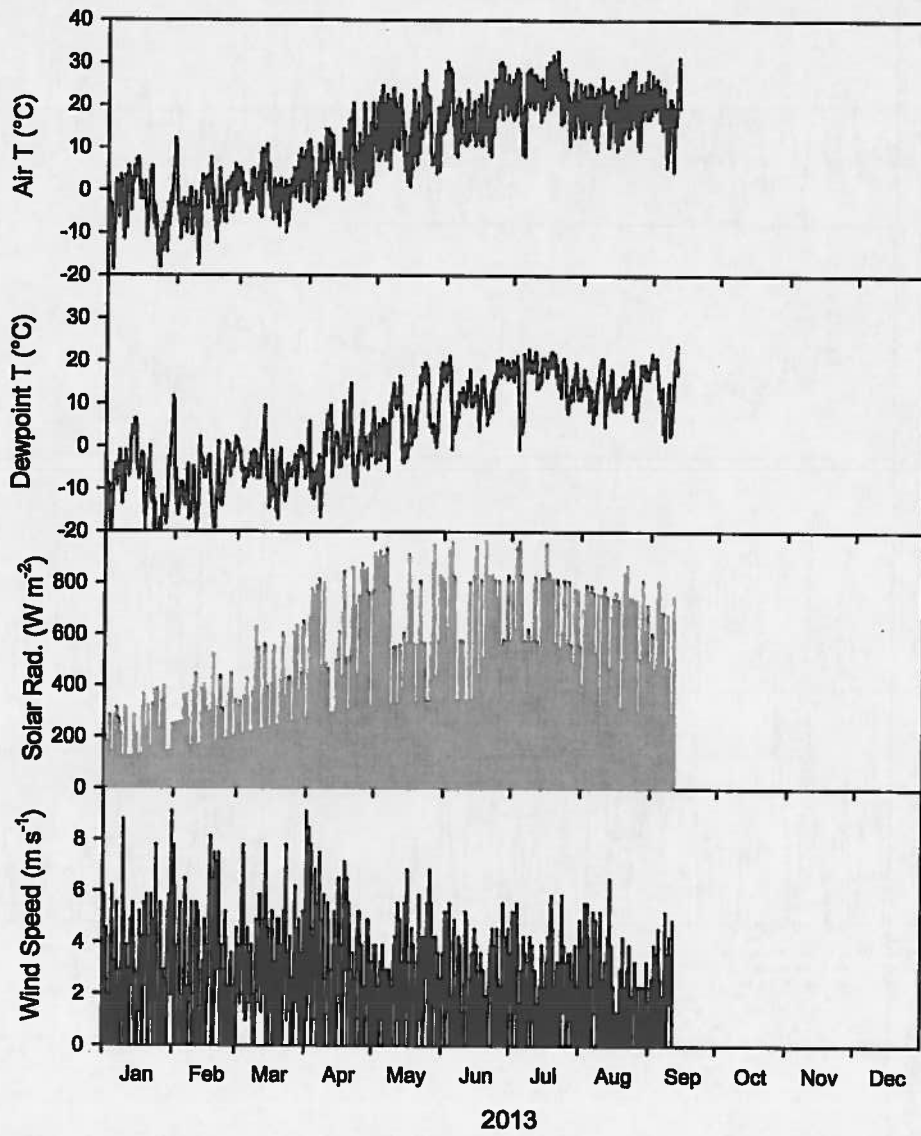


Figure 19. Meteorological data from Albany Airport adjusted for onsite conditions for 2013: Air temperature, dewpoint temperature, solar radiation (estimated from cloud cover), and wind speed.

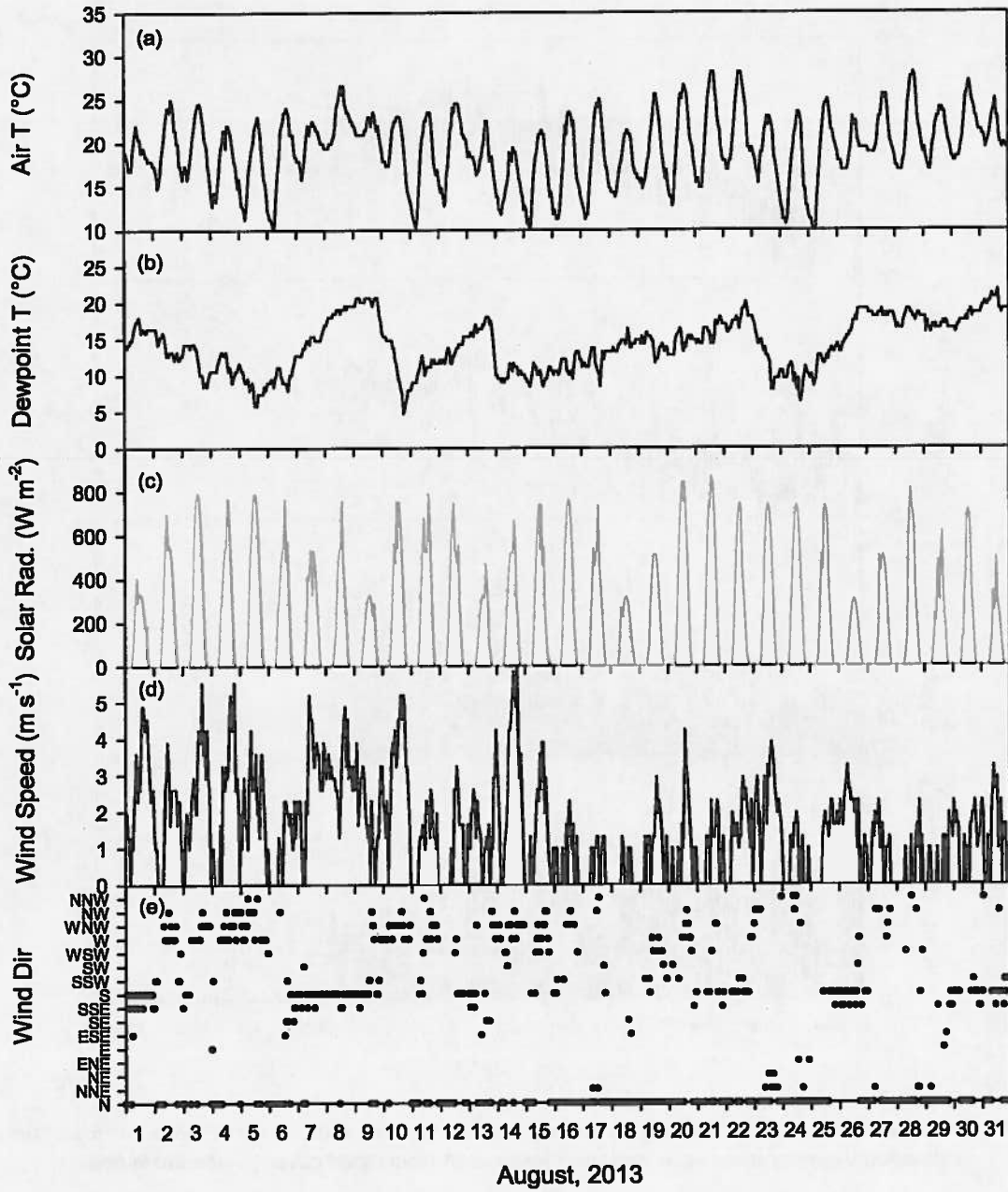


Figure 20. Meteorological data from Albany Airport adjusted for onsite conditions for August 2013: Air temperature, dewpoint temperature, solar radiation (estimated from cloud cover), wind speed, and wind direction.

4.2. Model Results

Model output of in-reservoir temperatures was saved every 15 minutes, whereas the withdrawal temperatures were saved every hour. The high temporal resolution of the model output allowed a more accurate comparison with the observations, and preservation of the intra-day oscillations in the withdrawal. Predictions of in-reservoir temperatures at selected sites are compared with the observations in the format of depth-profiles (Figures 21–23). The model continued to simulate well both the temporal and spatial temperature patterns in the reservoir (Figures 21–23), consistent with the prior application (Gelda and Effler 2007).

An important aspect of this work was to test the model's ability to reproduce observed oscillations in the withdrawal temperature. A comparison of the observed and predicted withdrawal temperatures for July–August, 2013, at SRR1 and SRR2 is shown in Figure 24a, and Figure 24b, respectively. Predictions for SRR2 site are the same as for SRR1 site except they are adjusted for the time of travel in Shandaken Tunnel (~ 8 hours for the prevailing withdrawal rate; Ganett Fleming and Hazen & Sawyer, 2009). The model did produced oscillations and tracked the central values of withdrawal temperatures fairly well; however, the amplitude of the oscillations was underpredicted. The daily average observed ranges (i.e., maximum – minimum) were 3.1 °C (SRR1) and 2.7 °C (SRR2), as compared to the predicted value of 1.6 °C. Uncertainty in the predictions may be due to one or more of the following factors: (i) empiricism in the selective withdrawal algorithm, (ii) 3-D features of the bathymetry in the vicinity of the intake affecting the local flow dynamics that is not represented in the 2-D framework of the model, and (iii) wind speed not representative of the local conditions. A brief discussion of these factors follows:

The selective withdrawal algorithm is based on empirically estimating a withdrawal zone first and then determining velocities of withdrawal in the withdrawal zone using a quadratic shape function (Cole and wells 2011). The algorithm does not consider local bathymetric features or geometry of the intake structure, which may influence the proportion of the water withdrawn from different layers as well as the zone of withdrawal itself.

The 3-D features of the bathymetry in the vicinity of the intake are a deep narrow channel along the western shore and a broad shelf (shallow waters) that covers most of the model segment with the intake structure (see Figure 6). The greater than the model-predicted range of oscillations of withdrawal temperatures suggest that (i) the actual withdrawal zone is probably more dynamic than the predictions, and (ii) the presence of narrow channel along the shore near the intake may cause transport of water directly from the upstream or downstream segments in the lower layers in response to internal waves (Anohin et al. 2006). The withdrawal zone in the format of depth profiles of selective withdrawal flow rate (Q_{sw}) is depicted in Figure 25. The maximum withdrawal is from the layers 1–2 m above the intake location, the lower boundary of the withdrawal zone is at the bottom of the model segment, and the upper boundary is near the lower epilimnetic layers (Figure 25). Cooler (than the predicted) withdrawal temperatures would be possible if the internal wave moved the water layers of the cooler temperatures (i.e., upward deflection of the isotherms at the windward end) into the withdrawal zone and near the maximum Q_{sw} . Similarly, warmer withdrawal temperatures would be possible if the

internal wave moved the water layers of the warmer temperatures (i.e., downward deflection of the isotherms at the windward end when the wind force ceases) into the withdrawal zone and near the maximum Q_{sw} . A 3-D model would also simulate the transport of the cooler water from the downstream segment and the warmer water from the upstream segment into the withdrawal zone due to internal wave more accurately (Anohin et al. 2006).

Lastly, the uncertainty in the wind speed may have contributed to the amplitude of the internal waves affecting the predictions of the range of oscillations in the withdrawal temperatures. As noted earlier, the wind speed measurements were made at nearby Albany Airport and adjusted to onsite conditions. There were no direct onsite measurements of wind available for the period of simulation.

4.3. Analysis of Predicted Isotherms

Further insight into the interplay of stratification, wind, and internal waves can be gained by examining isotherms at the intake (site 3) and dam (site 1) locations. The model output was interrogated to report timeseries of depths of selected isotherms at the two sites for August 1–14, 2013 interval. Considerable fluctuations of the temperatures with respect to depth are predicted (Figure 26). Figure 26 illustrates the variations in the depths of the 12°, 13°, 15°, 17°, and 19 °C isotherms at site 3 (Figure 26b), and at site 1 (Figure 26c). Depth range of 10–12 m corresponds to the metalimnetic layers. The north-south components of the wind for the same period are shown in Figure 26a.

The coupling of the wind stress and the internal wave as reflected in the sinusoidal wave like motion of the isotherms is evident for the southerly wind inputs of August 1 and August 7. During the application of the wind stress (August 1; Figure 26a), the isotherms at the intake site (windward end) are deflected upward (Figure 26b), demonstrating the movement of the warmer waters to the shallower depths. When the wind gradually ceases, the internal wave ‘rocks’ in the opposite direction deflecting the isotherms downward indicating transport of the warmer waters to the deeper depths (Figure 26b). The gradual dampening of the internal wave is demonstrated with the reduction in the amplitude of the variations (e.g., see 12 °C isotherm, from August 1–6, Figure 26b). Blowing from south, wind speed increases ($\sim 4 \text{ m s}^{-1}$) again on August 7 (Figure 26a), which renews the internal wave and the amplitude increases again. At the leeward end near the dam, the opposite behavior of the isotherms is predicted in response to the wind stress input (Figure 26c). Additionally, higher mode internal waves may be present as shown by the out of phase predictions of 10 °C and 19 °C isotherms (August 1–3; Figure 26c) near the dam.

The spectral analysis of the 15 °C isotherm (Figure 27) from site 3 for August 1–6 shows three dominant periodicities at 32 hr, 22 hr, and 15 hr, indicating operation of three distinct interacting waves. The periods of the two of these waves, 22 hr and 15 hr, matched exactly with the periods observed in the temperature timeseries at SRR1 for the same time interval (Figure 17). The spectra for SRR1 temperature did not indicate the low frequency 32 hr period wave.

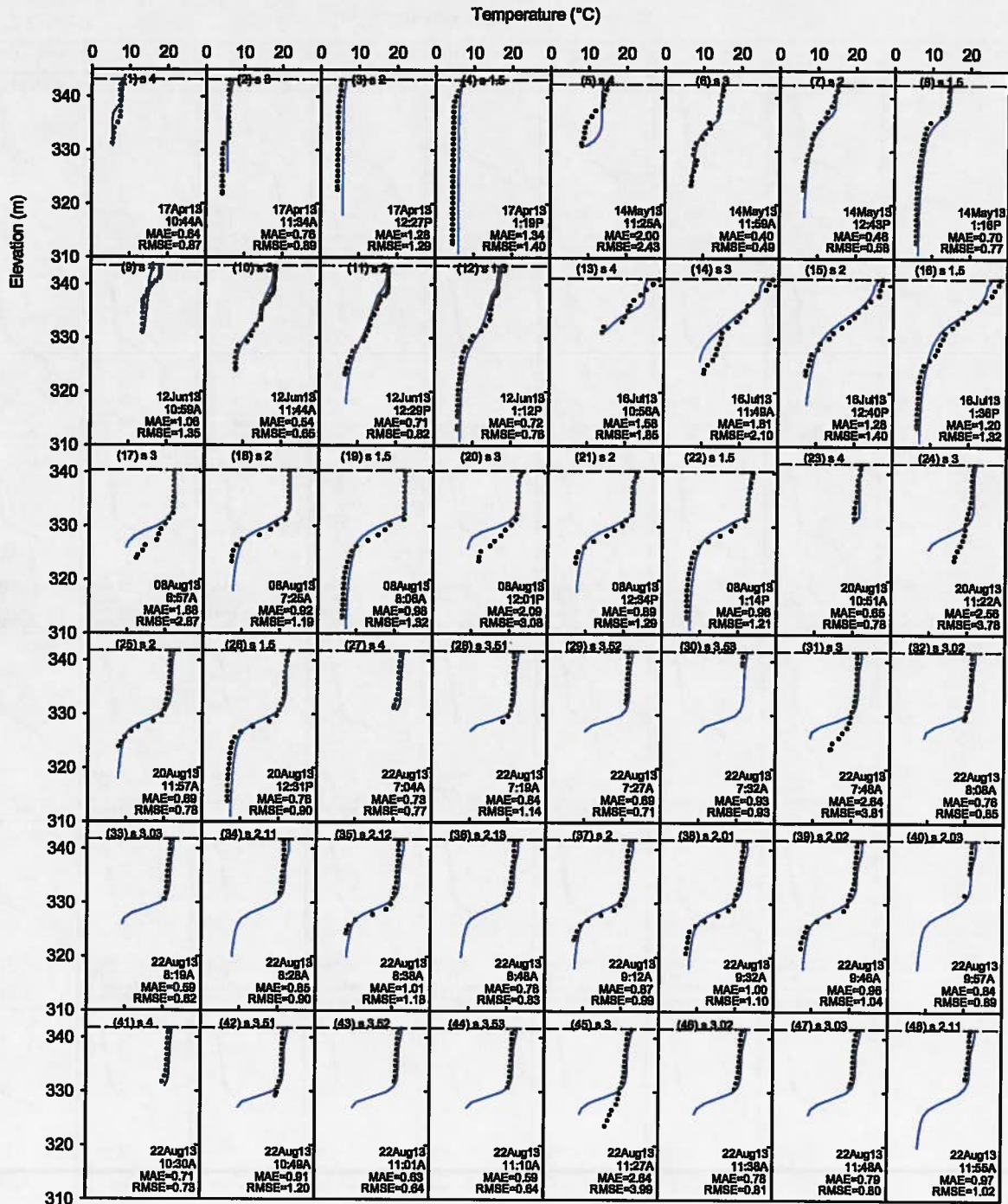


Figure 21. Comparison of the observed (symbols) and the model-predicted (lines) temperature profiles at selected locations in Schoharie Reservoir for April 17–August 22, 2013 interval.

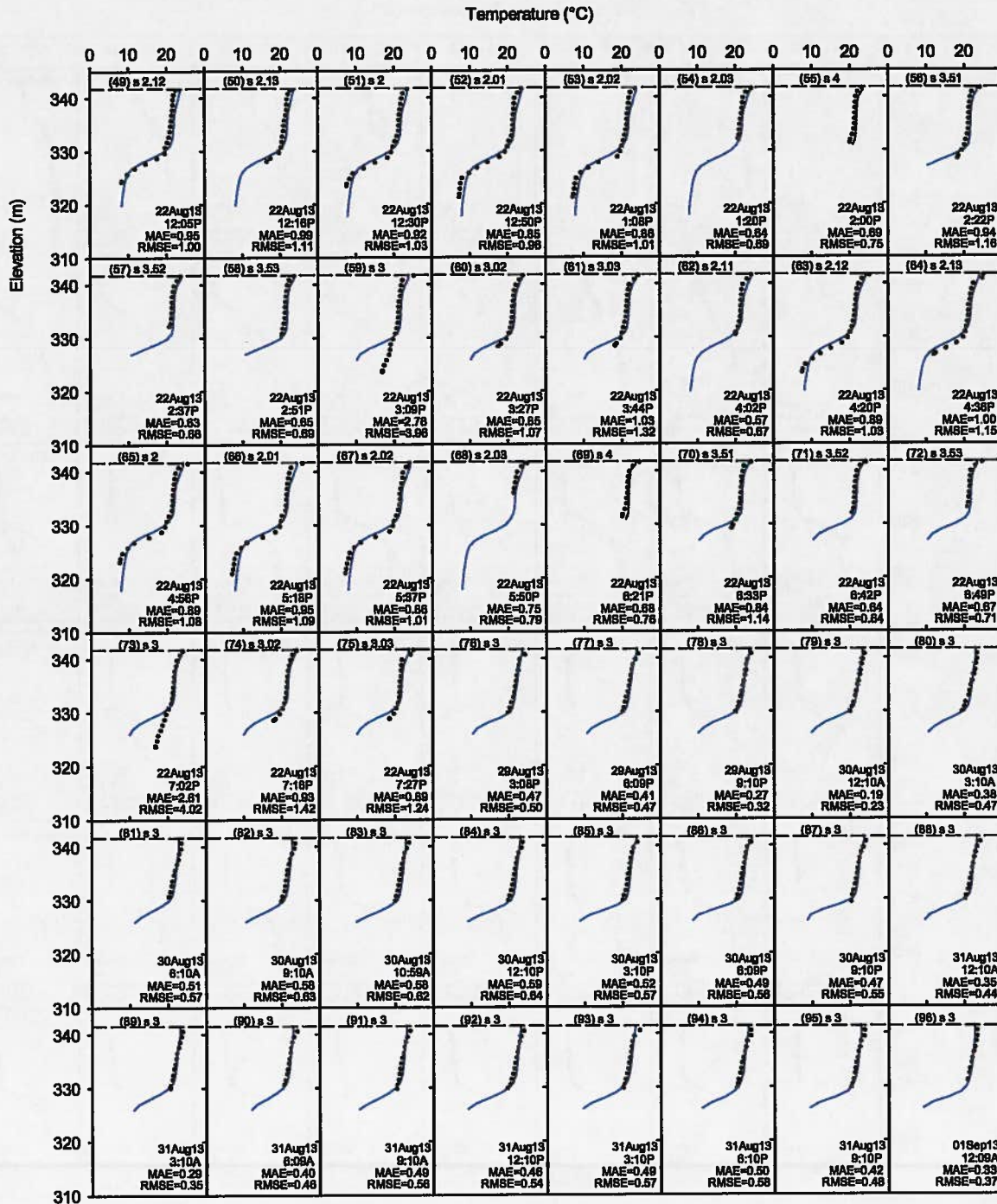


Figure 22. Comparison of the observed (symbols) and the model-predicted (lines) temperature profiles at selected locations in Schoharie Reservoir for August 22–September 1, 2013 interval.

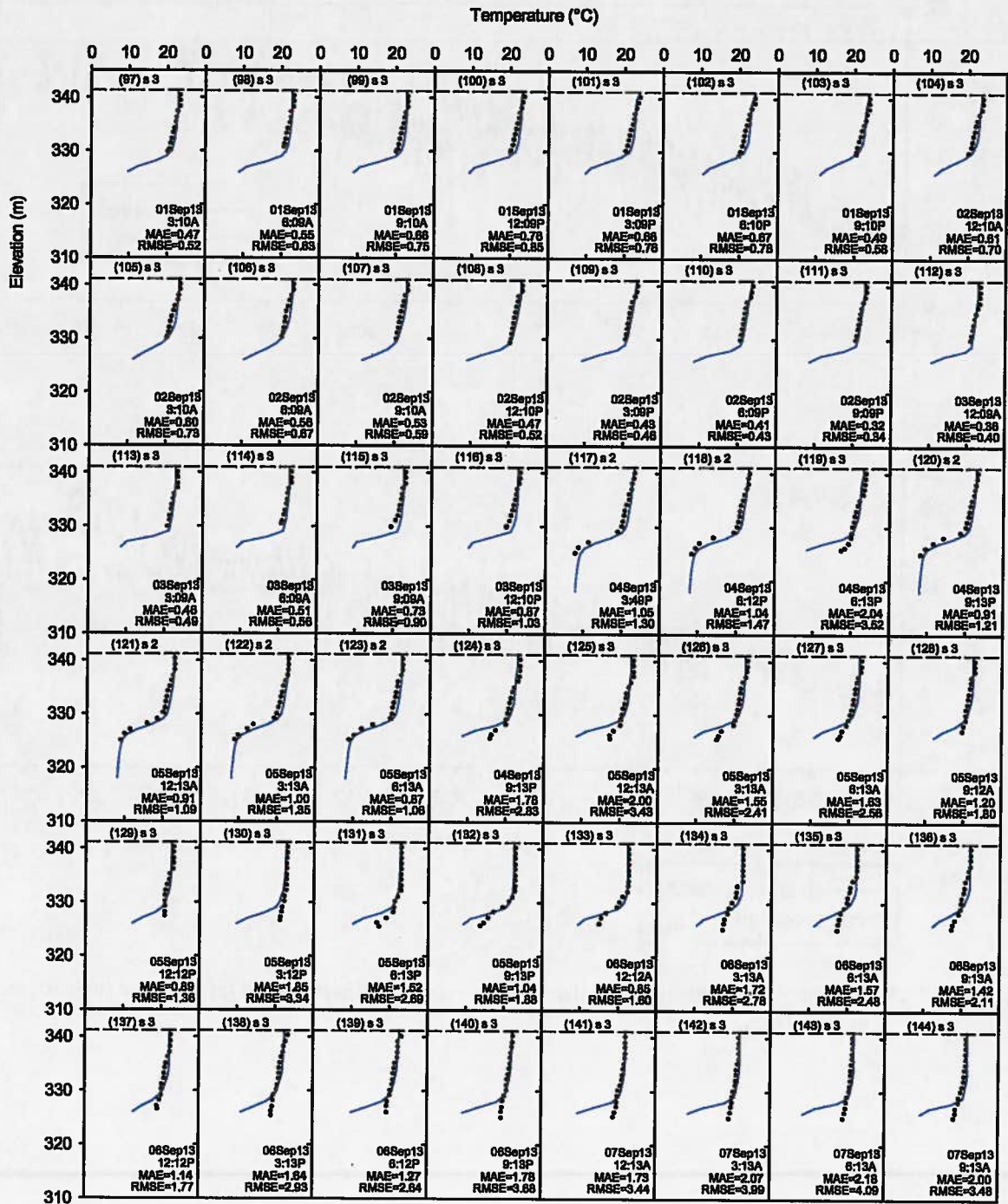


Figure 23. Comparison of the observed (symbols) and the model-predicted (lines) temperature profiles at selected locations in Schoharie Reservoir for September 1–September 7, 2013 interval.

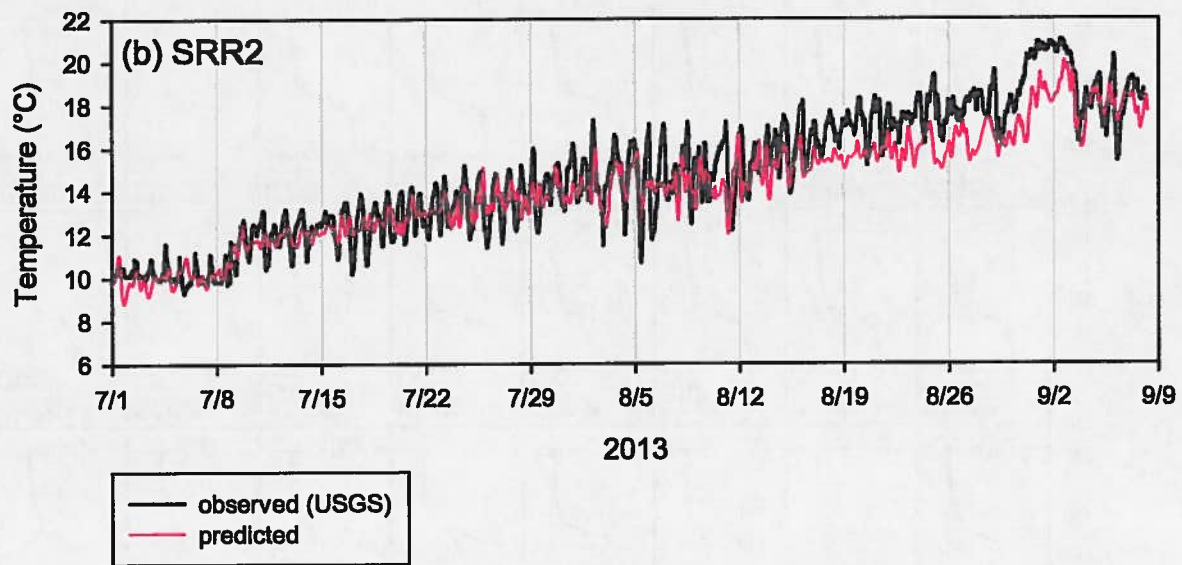
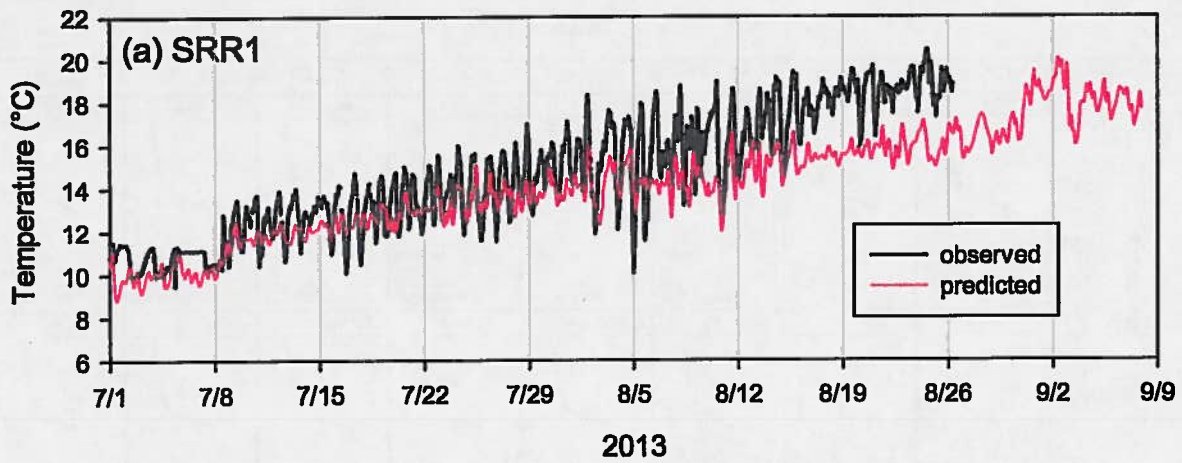


Figure 24. Comparison of the observed and the model-predicted temperatures at (a) SRR1 and (b) SRR2, for July–August, 2013.

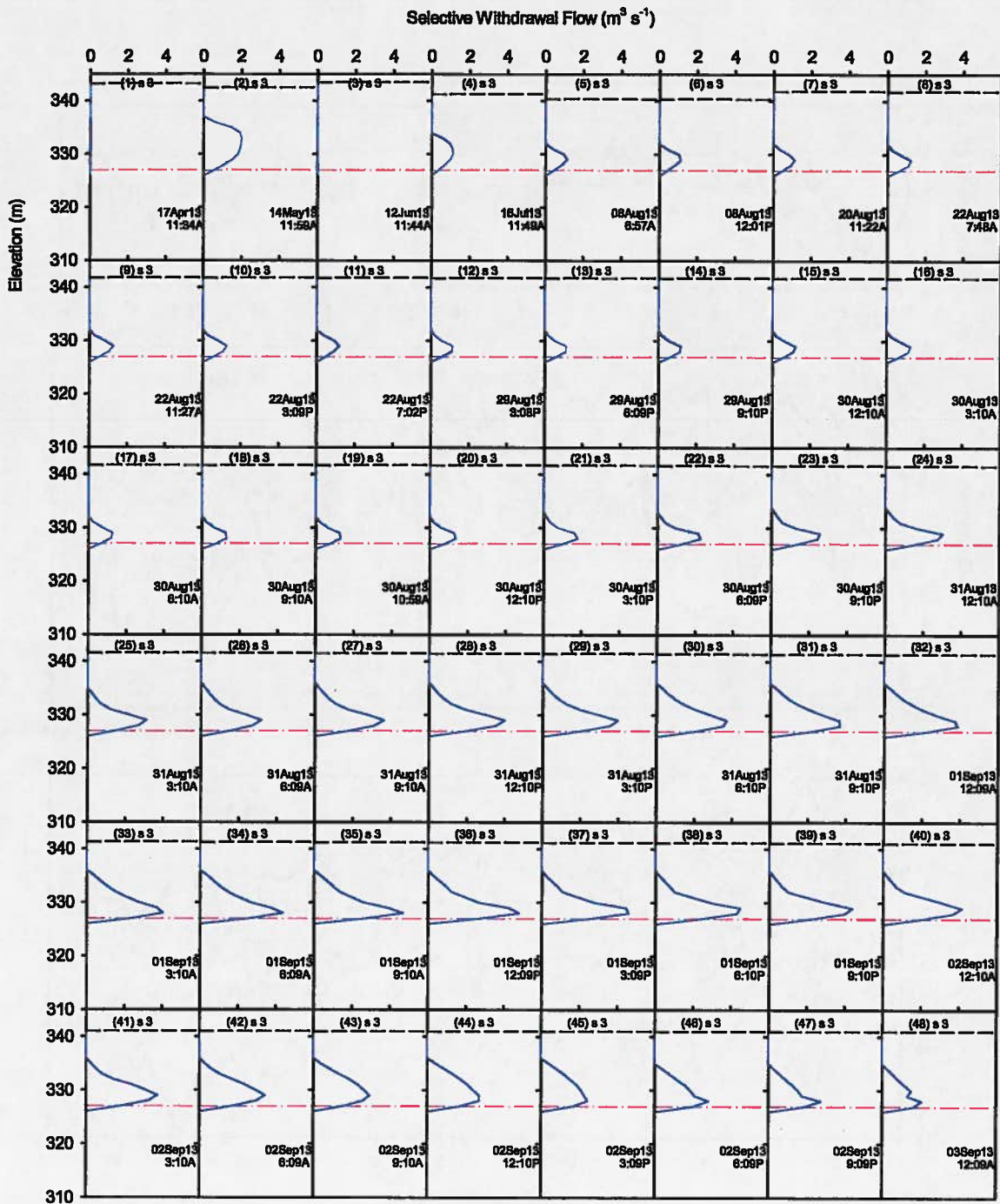


Figure 25. Model-predicted withdrawal zone in the format of depth profile of selective withdrawal flow rate on the days of collection of temperature profiles at site 3. Intake elevation is indicated by red line.

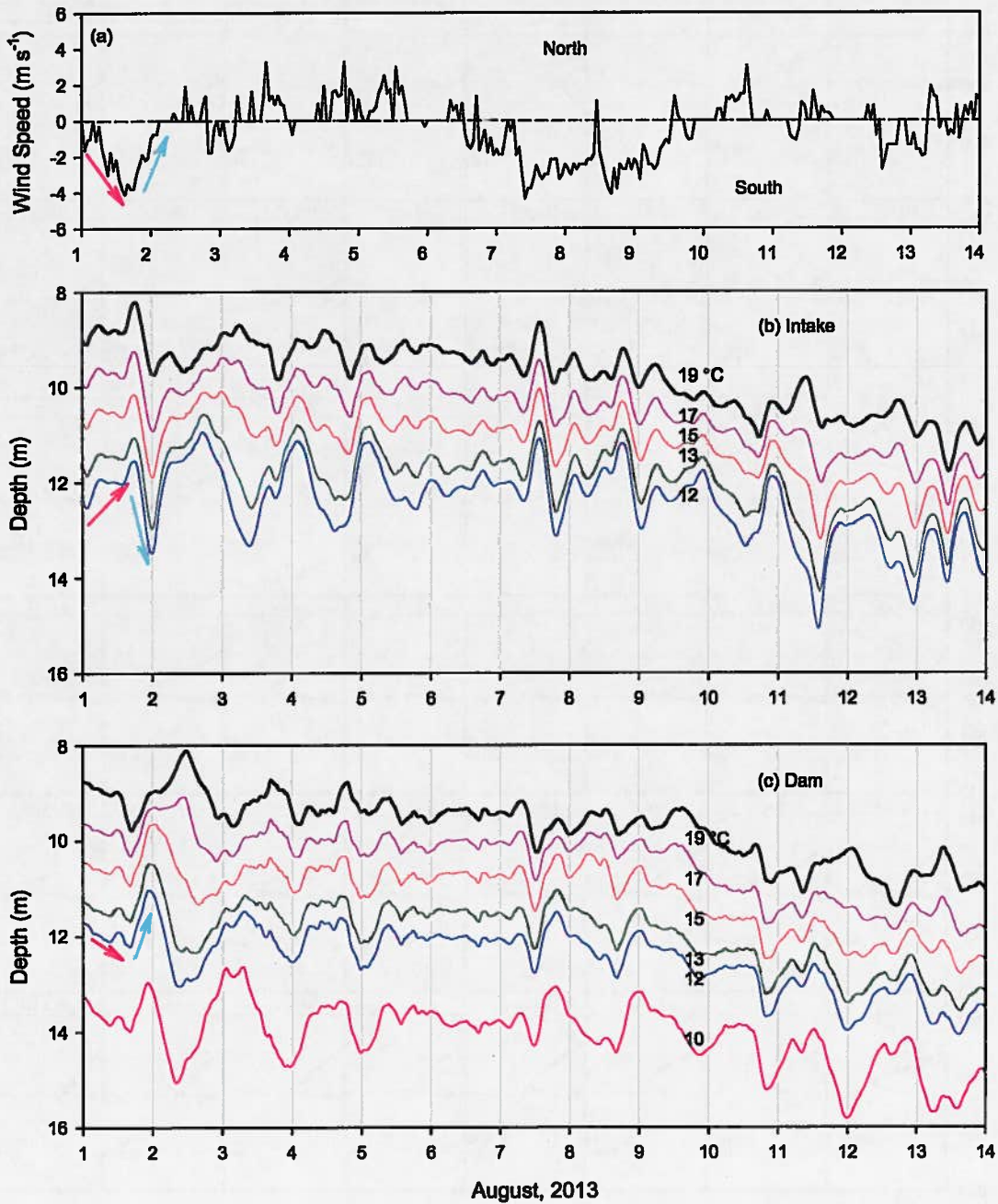


Figure 26. (a) North-south components of wind speed for August 2013, (b) depth oscillations of predicted 12°, 13°, 15°, 17°, and 19° C isotherms in Schoharie Reservoir at Intake site, and (c) depth oscillations of predicted 10°, 12°, 13°, 15°, 17°, and 19° C isotherms in Schoharie Reservoir at dam site. Arrows indicate deflection of isotherms in response to rising and falling wind speed.

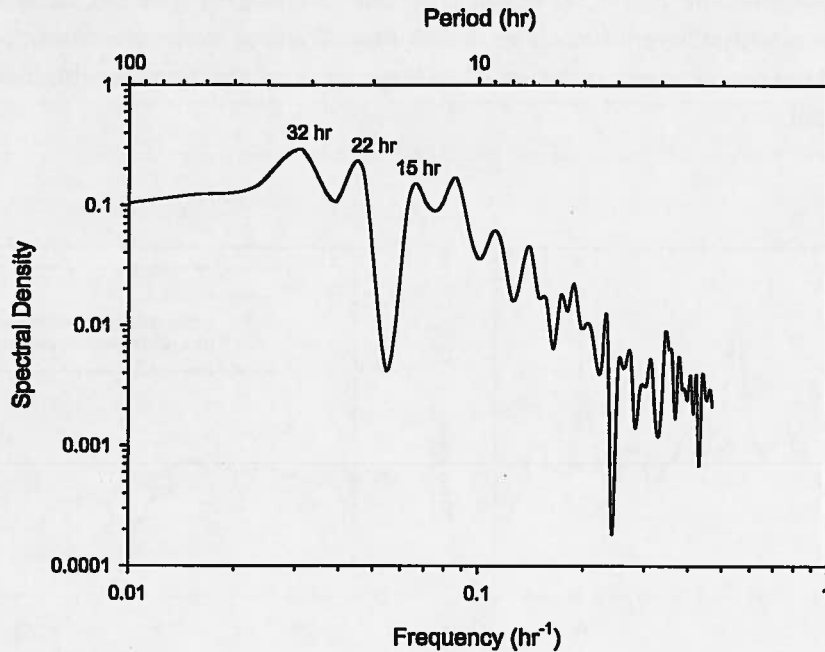


Figure 27. Spectra for the model-predicted 15 °C isotherm, for August 1–6, 2013, at site 3.

4.4. Withdrawal Turbidity

Calculation from modeled selective withdrawal flow and observed in-reservoir turbidity profiles:

The presence of internal waves in the reservoir can also explain the rapid fluctuations seen in the withdrawal turbidity (Figure 2b). Strong stratification in turbidity existed as shown by the depth-profiles at site 3 for August 22, 2013 (Figure 8a). Average turbidity in the upper mixed layer (0–10 m depth) was 4 NTU as compared to 41 NTU in the lower (11–18 m depth) stratified layers (Figure 8a). Due to internal waves, a modest upward and downward tilt of the thermocline, at ~ 11 m, moves layers of high and low turbidities in the withdrawal zone resulting in fluctuations in the overall withdrawal turbidity.

Calculations of the withdrawal turbidity were done for the two in-reservoir turbidity profiles collected on August 8, and two on August 22, 2013, at site 3, using modeled selective withdrawal flows (Figure 25) and observed turbidity profiles, according to:

$$T_{n,w} = \frac{\sum_{i=1}^N Q_{sw,i} T_{n,obs,i}}{Q_w} \quad (6)$$

where, $T_{n,w}$ = withdrawal turbidity (NTU); $Q_{sw,i}$ = modeled selective withdrawal flow for i^{th} layer ($m^3 s^{-1}$); N = number of layers in the withdrawal zone; $T_{n,obs,i}$ = observed turbidity for i^{th} layer at site 3 (NTU); and

Q_w = overall withdrawal flow ($\text{m}^3 \text{s}^{-1}$). The computed withdrawal turbidities were lower for August 8; however, it matched well for August 22, including the diurnal change (Figure 28). Besides selective withdrawal of layers with different turbidities due to internal waves, horizontal currents associated with these waves, and the presence of benthic nephroid layer may contribute to the withdrawal water quality (Anohin et al. 2006).

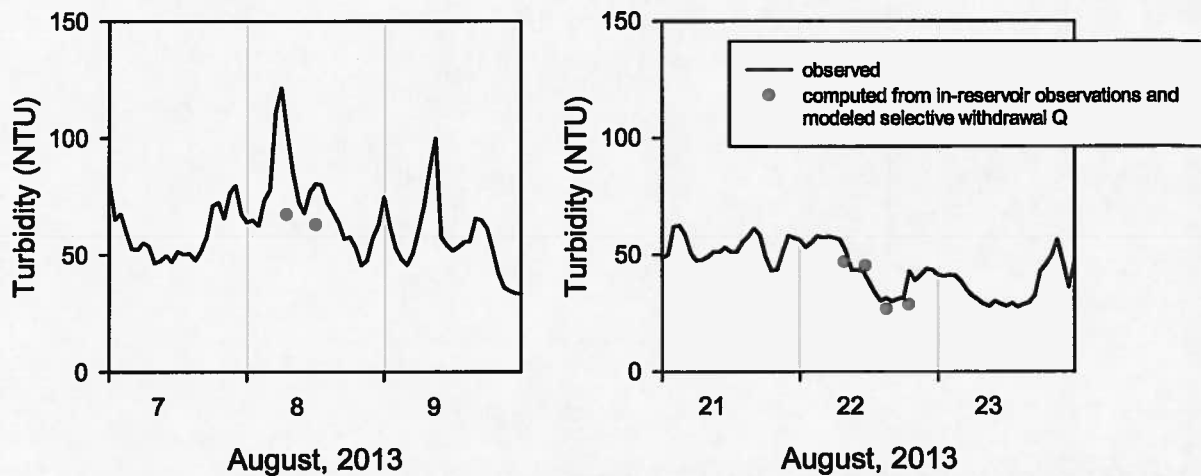


Figure 28. Comparison of the observed (solid line) and computed withdrawal turbidity (circles), for the days of turbidity depth-profiles monitored at site 3.

Simulation using estimated turbidity loading from Schoharie Creek:

The model was also setup to simulate turbidity in the reservoir and in the withdrawal for the study period. Because of very limited measurements of turbidity in the Schoharie Creek input, a flow-turbidity relationship (Gannett Fleming & Hazen and Sawyer 2009) was used to estimate turbidity loading. As shown in Figure 29, Schoharie Creek was not a significant source of turbidity during July–August, 2013; however, there was a storm event in mid-June when the peak turbidity was estimated to be 190 NTU. Model performance is evaluated in terms of the epilimnetic and hypolimnetic average turbidity at site 3, and withdrawal turbidity. The predicted turbidities were lower than the observed in both the epilimnion and hypolimnion (Figure 30). The difference was larger in the hypolimnion than in the epilimnion. The possible causes of underprediction in the epilimnion include uncertainty in the estimates of loading from Schoharie Creek, and absence of surface wave driven resuspension, whereas absence of resuspension driven by the seiche-induced horizontal currents is the likely cause of underprediction of turbidity in the hypolimnion. Model-predicted withdrawal turbidities at SRR2 are also lower than the observed for July–August interval (Figure 31); likely due to the same reasons as stated for the in-reservoir turbidity predictions. It is recommended that the future turbidity modeling work on Schoharie Reservoir include developing a quantitative framework of seiche-induced resuspension in the reservoir, and assess its contribution to the overall turbidity.

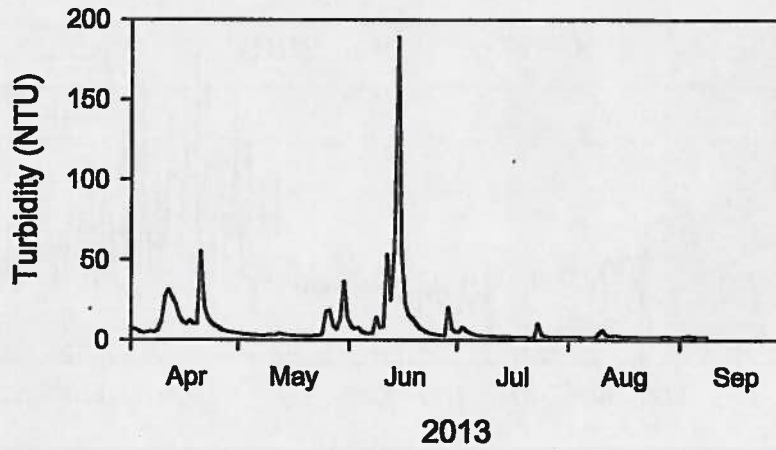


Figure 29. Schoharie Creek turbidity estimated from a flow-turbidity relationship (Gannett Fleming & Hazen and Sawyer 2009) for 2013.

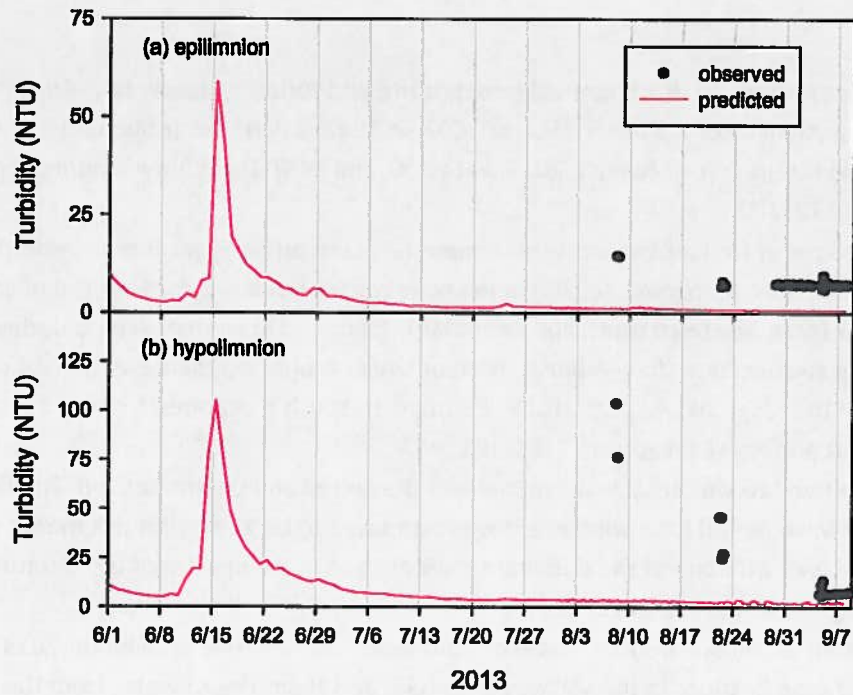


Figure 30. Comparison of the observed and the model-predicted turbidity in (a) epilimnion and (b) hypolimnion, at site 3 in Schoharie Reservoir.

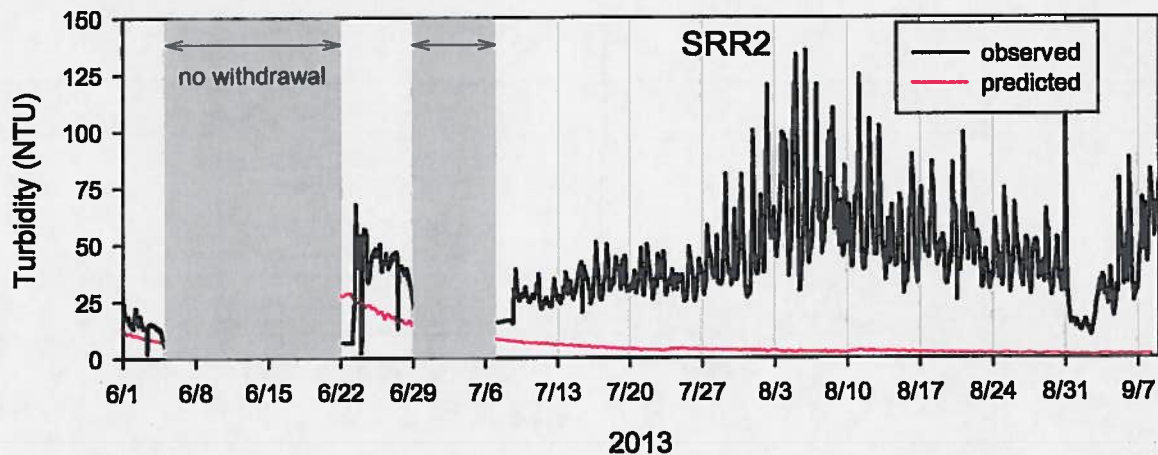


Figure 31. Comparison of the observed and the model-predicted turbidity at SRR2 for June–August, 2013. Shaded area indicate interval of no withdrawal.

5. Summary and Conclusions

- Oscillations observed in withdrawal temperature and turbidity during July–August 2013 are recurring. Analysis of historical data for 2007–2012 revealed similar fluctuations. Average daily fluctuations during July–August, 2013 were 3 °C, and 34 NTU, with maximum fluctuations being 8 °C and 112 NTU.
- Observations of frequent short-term temperature and turbidity profiles provide the evidence of an internal wave (baroclinic seiche) in the reservoir. Periodic winds along the main axis of the reservoir (primarily from south and secondarily from north) were observed during the intervals of strong stratification (July–August), both of which supported the development of internal waves in the reservoir. A spectral analysis of north-south components of wind suggested several dominant periods ranging from 1 d to 6 d.
- A simple two-layer internal wave model was presented and parameterized. The first-mode internal wave period for a wind event was estimated to be 15 hr with this model, which matched well with one of the dominant periods seen in the spectra of temperature timeseries, following the wind event, at SRR1.
- A validated 2-D hydrothermal model of Schoharie Reservoir was applied for 2013 data that also included modifications in the spillway (v-notch), and siphoning of water from the model segment adjoining the dam. The model performed well in simulating in-reservoir temperature profiles. The model also predicted the observed oscillations in the withdrawal temperatures; however, the amplitude of the oscillations was underpredicted.
- Selected model-predicted isotherms were analyzed for internal waves. Deflections of the isotherms in response to wind events are predicted to be consistent with the internal wave

activity. The spectral analysis of one of the isotherms from site 3 showed dominant periods that matched exactly with the periods observed in the temperature timeseries at SRR1.

- The sources of uncertainties in the 2-D model were identified as follows: 3-D features in the bathymetry of the reservoir in the vicinity of the intake and associated local flow dynamics, lack of onsite wind measurements, and empiricism in the selective withdrawal algorithm.
- Future work may include testing of the 2-D model for additional years (e.g., 2007-2012), evaluation of the SPDES permit for Shandaken Tunnel discharge into Esopus Creek in light of recurring short-term oscillations in temperature and turbidity of the discharge, and installing automated monitoring systems in the reservoir and Schoharie Creek. Of particular interest may be the application of the model for 2007-2012 years to further understand the phenomenon of seiche-induced resuspension and possibly address in the model in a semi-empirical manner through calibration.

6. References

Anohin, V. V., J. Imberger, J. R. Romero and G. N. Ivey. 2006. Effect of long internal waves on the quality of water withdrawn from a stratified reservoir. *Journal of Hydraulic Engineering* 132:1134-1145.

Carmack, E. C., R. C. Wiegand, R. J. Daley, C. B. Gray, S. Jasper and C. H. Pharo. 1986. Mechanisms influencing the circulation and distribution of water mass in a medium residence-time lake. *Limnol. Oceanogr.* 31:249-265.

Cole, T. and S. A. Wells. 2011. CE-QUAL-W2: A Two-Dimensional, Laterally Averaged, Hydrodynamic and Water Quality Model, Version 3.71, Instruction Report EL-2011-1. Department of Civil and Environmental Engineering, Portland State University, Portland, Oregon.

Effler, S. W., B. A. Wagner, D. M. O'Donnell, S. M. O'Donnell, D. A. Matthews, R. K. Gelda, C. M. Matthews and E. A. Cowen. 2004. An upwelling event at Onondaga Lake, NY: Characterization, impact and recurrence. *Hydrobiologia* 511:185-199.

Fischer, H. B., E. J. List, J. Imberger, R. C. Koh and N. H. Brooks. 1979. *Mixing in inland and coastal waters.* Academic Press, NY.

Gannett Fleming & Hazen and Sawyer. 2009. Catskill turbidity control studies: Phase II Implementation Plan - Updates and Supporting Analyses. Prepared for New York City Department of Environmental Protection, Bureau of Engineering Design and Construction.

Gelda, R. K. and S. W. Effler. 2007. Testing and application of a two-dimensional hydrothermal model for a water supply reservoir: Implications of sedimentation. *Journal of Environmental Engineering and Science* 6:73-84.

Gelda, R. K. and S. W. Effler. 2008. Probabilistic model for temperature and turbidity in a reservoir withdrawal. *Lake and Reservoir Management* 24:219-230.

Imberger, J. 1985. The diurnal mixed layer. *Limnol. Oceanogr.* 30:737-770.

Martin, J. L. and S. C. McCutcheon. 1999. *Hydrodynamics and transport for water quality modeling.* Lewis Publishers, Boca Raton, FL. 794 p.

Monismith, S. G. 1986. An experimental study of the upwelling response of stratified reservoirs to surface shear stress. *Journal of Fluid Mechanics* 171:407-439.

Mortimer, C. H. 1952. Water movements in lakes during summer stratification: Evidence from the distribution of temperature in Windermere. *Trans. R. Soc. London Ser. B* 236:353-404.

Mortimer, C. H. 1961. Motion in thermoclines. *Verh. Internat. Verein. Theor. Angew. Limnol.* 14:79-83.

Spigel, R. H. and J. Imberger. 1980. The classification of mixed layer dynamics in lakes of small to medium size. *J. Physical Oceanogr.* 10:1104-1121.

Stevens, C. L. and G. A. Lawrence. 1997. Estimation of wind-forced internal seiche amplitudes in lakes and reservoirs, with data from British Columbia, Canada. *Aquatic Science* 59:115-134.

Upstate Freshwater Institute. 2013. Memo: Meteorological data regressions for Schoharie Reservoir. Submitted to NYCDEP.

Wetzel, R. G. 2001. *Limnology: lake and reservoir ecosystems.* Academic Press, New York.

White, F. M. 1998. *Fluid Mechanics*, 4th ed. McGraw-Hill, New York.